Homogenization of solid-electrolyte composite intercalation cathodes for energy storage systems

Markus Schmuck

Homogenization of solid-electrolyte composite intercalation cathodes for energy storage systems

Markus Schmuck*

Maxwell Institute for Mathematical Sciences
and School of Mathematical and Computer Sciences
Department of Mathematics
Heriot-Watt University
Edinburgh, EH144AS, UK

March 8, 2017

Abstract

We investigate well-accepted formulations describing charge transport in composite cathodes of batteries. Our upscaling of carefully selected microscopic equations shows three main features:

(i) a novel set of six equations equipped with nine effective parameters which systematically couple the microscale to the macroscale;

(ii) the coupling of transport and flow equations allows to account for three scales: pore scale, Darcy scale, and macroscale;

(iii) the upscaled equations take phase separation during Li-intercalation into account as well as specific particle configurations.

The wide range of applications and interest in energy storage devices make these results a promising tool to study the influence of the microstructure on current-voltage characteristics and to optimize cathode designs.

Keywords: batteries, homogenization, current-voltage curves, lithium intercalation, phase separation, Butler-Volmer reactions

1 Introduction

We look at basic and widely accepted equations describing charge transport and reactions in composite cathode materials of energy storage systems such as Li-batteries. The main goal of this article is to systematically and reliably derive effective macroscopic equations that account for characteristic material properties such as geometric features of interfaces and material phases as well as electric and ionic conductivities and reaction rates. In particular, the subsequent mathematical modelling shall help to gain a deeper understanding into how material properties influence experimentally measured current-voltage characteristics. With the introduction of $LiFePO_4$ as a promising cathode material in 1997, strong improvements in charging and discharging rates as

*M.Schmuck@hw.ac.uk (corresponding author)

well as in safety have helped to make phosphates a promising battery material [22]. A crucial role for the charging and discharging rate plays the so-called Li-intercalation in which Li-ions enter into crystalline phosphate particles of the composite cathode. During this process, the phosphate material can phase separate into a Li-rich phase and a Li-poor phase for which a first modelling seems to be [21]. Previous formulations describe the intercalation by a shrinking core using radial diffusion [14]. Crystalline intercalation compounds show a topotactic transition, i.e., the compound may change its structure due to gain or loss of material (which is Li here). Recent research suggests that a change in structure/phase separation can be suppressed in $LiFePO_4$ nanoparticles, e.g. [4]. Suppression can occur in equilibrium [30], but when a current flows [28], non-idealities are enhanced and hence the suppression seems even more likely. This leads immediately to the important and interesting question what influence can the mircro-geometry have on the appearance of phase separation in these composite cathodes and on the current-voltage characteristics. For instance, it is possible that different parts of the composite cathode are in a different state and hence phase separation can be expected to be a very local property over time. In order to better understand the key properties of composite cathodes for optimizing design and safety, systematic mathematical and thermodynamic modelling will play a crucial role towards a reliable, effective macroscopic description of intercalation kinetics of Li^+-ions into solid particles such as $FePO_4$.

Existing porous electrode theory for batteries relies on intuitive, formal, or ad hoc averaging strategies based on integrating the equations directly over a representative volume element [4, 19, 48]. This kind of intuitive averaging seems to take dominant transport characteristics such as porosity and surface area into account but generally neglects more subtle geometric features such as pore shape and properties that go beyond porosity and tortuosity characterisations. Currently, it is still an open question how to rigorously justify the volume averaging approach. Often, these methods are refined with physically derived corrections to transport coefficients. Famous porous media corrections to transport parameters are the so-called Bruggeman relation [7], i.e., the diffusion coefficient D_p of the pore phase is obtained by multiplying the free space diffusion parameter D_f by the factor $p^{3/2}$ where p is the porosity. More refined relations also take the tortuosity into account [49], i.e., $D_p = 1/\tau D_f$. The parameter τ is the tortuosity defined as the quotient $\tau := \frac{L_a}{L_s}$ where L_a is the length of the actual transport path through the pore and L_s is the shortest distance connecting entrance and exit of a reference pore. There is increasing interest in the context of ionic transport to systematically derive upscaled/homogenized equations [2, 25, 38, 42, 43, 45]. For fuel cell and battery systems recent upscaling results are [20, 26, 39, 46] for instance. A summary of work closely related to the results presented in this article is given in Tab. 1. Due to increasing interest and number of publications, we do not claim this table to be complete.

Besides a wide interest in thermodynamics and materials science, the highly heterogeneous and multiphase character of composite cathodes requires a systematic and reliable derivation of effective macroscopic transport equations taking physically observed principles as well as geometric features of the microscale into account while still allowing for feasible and efficient computational schemes. The homogenization of charge transport equations in cathodes is the main goal of this article. The basic idea in homogenization is to account for at least one smaller length scale $\ell \ll L$, the so-called microscale $\mathbf{y} = \frac{\mathbf{x}}{\ell} L \in Y \subset \mathbb{R}^d$, which takes geometric features such as pore shape or changing material properties such as electric permittivity/conductivity into account. The parameter L is the macroscale (e.g. length of the composite cathode) such that $\epsilon = \frac{\ell}{L}$ represents the material's heterogeneity. The microscale is identified by a periodic reference cell (periodic homogenization). Homogenized equations can then be obtained by applying a so-called asymptotic

Table 1: Summary of derivations of effective macroscopic equations for battery systems with Li-intercalation. The fact that the majority of work relies on volume averaging can be in part motivated by the fact that this intuitive method is more formal as it does not require rigorous existence and uniqueness results in the derivation like the asymptotic two-scale expansion applied here. Due to an increasingly growing literature on Li-battery modelling over the last decade, we do not claim this list to be complete.

Article	**Volume averaging**	**Homogenization**
Doyle et al. 1993, [14]	• concentrated solution • Butler-Volmer reactions • Bruggeman relation • full battery model	
Han et al. 2004, [21]	• "phase field" intercalation • only intercalation modelling	
Garcia et al. 2005, [19]	• Nernst-Planck transport • stress due to volume change • Butler-Volmer reactions • model validation	
Lai et al. 2011, [26]	• comparing Nernst-Planck & concentrated solution • Bruggeman relation	
Hautier et al. 2011, [22]	• ab initio investigation of phosphate cathode materials	
Richardson et al. 2012, [39]		• Nernst-Planck transport • Butler-Volmer reactions • "fast diffusion" intercalation • no flow
Bazant 2013, [4]	• "phase field" intercalation • single particle investigations • no flow • Butler-Volmer/ Marcus reactions	
Efendiev et al. 2013, [16]		• Nernst-Planck transport • "diffusive" intercalation • no flow • Butler-Volmer reactions
This article 2017		• Nernst-Planck transport • "phase field" intercalation • fluid flow • Butler-Volmer reactions

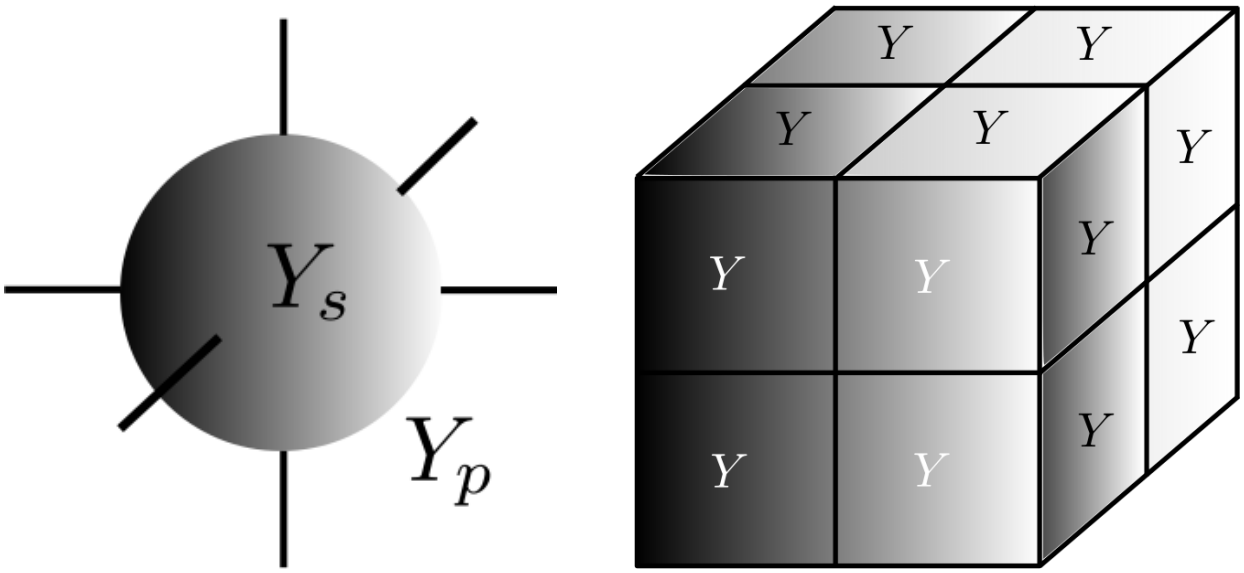

Figure 1: **Left:** Reference cell Y consisting of a polymer solution Y_p together with the solid intercalation compound Y_s, i.e., $Y = Y_p \cup Y_s$. The cell is electrically conducting due to the thin carbon black pathways connecting Y_s. **Right:** Reference cell Y_D, here for instance composed of an elementary pore cell Y such as depicted on the left-hand side. The cell Y_D takes the influence of obstacles to momentum transport into account. The union of the Y_p phases in Y_D are then denoted by Y_D^p and similarly Y_D^s represents the union of the Y_s phases in Y_D.

multiscale expansion of the form

$$u^\epsilon(\mathbf{x}) = u(\mathbf{x},\mathbf{y}) = u_0(\mathbf{x},\mathbf{y}) + \epsilon u_1(\mathbf{x},\mathbf{y}) + \epsilon^2 u_2(\mathbf{x},\mathbf{y}) + \cdots .$$

Then well-posedness theory allows us to identify the equations for u_0 and u_1 which represent the relevant terms in the upscaled/homogenized problem. This is a well-accepted methodology by now [10, 12, 23, 31].

We describe the composite cathode of lithium ion batteries together with available charge transport equations in Section 2. Then, we formulate the microscopic composite cathode model which we will subsequently upscale/homogenize and which fully resolves the different phases in Section 2.2. Based on well accepted charge transport models, we present the homogenized/upscaled charge transport equations for composite cathode materials in Section 3. A derivation based on the asymptotic two-scale expansion follows then in Section 3.1.

2 Microscopic composite cathode formulation

We consider a composite cathode which consists of solid intercalation particles $Y_s \subset Y := [0,1]^d$, $d \in \mathbb{N}$ dimension of space, and a polymer solution $Y_p \subset Y$ which together define a characteristic reference cell $Y := Y_p \cup Y_s$, see Fig. 1 (**Left**). Moreover, the particles Y_s are connected via thin carbon black pathways allowing for electron transport. We state the basic equations that account for charge transport in a composite as defined in the reference cell Y. We refer the reader not interested in an overview on available physical models directly to Section 2.2 where we formulate the microscopic starting point of our upscaling/homogenization derivation.

2.1 Basic physical processes and models

Before we look at the upscaling/homogenization of the composite cathode, we introduce models available in the literature to describe charge transport.

(S) Li-Intercalation compound/particles (solid matrix):
The intercalation particles show two different transport characteristics, i.e, electron transport and Li-intercalation into an electrochemical solid (subject to constraints such as charge and mass conservation, see [19] for instance.) The general atomic transport/diffusion mechanisms through solids are either by interstitial diffusion (defects in lattice where atoms assume a normally unoccupied site), vacancy diffusion (driven by thermal energy of atomic vibrations), or via impurities (interdiffusion driven by concentration gradients). Interstitial diffusion is generally faster than vacancy diffusion due to the higher number of interstitial sites and the weaker bonding of interstitials to neighbouring atoms. Since Li resides in interstitial sites, crystalline intercalation hosts such as $FePO_4$ are favourable for battery applications. We focus here on topotactic compounds, that means, hosts/particles that may change its structure due to gain or loss of material. As a consequence, the local Li concentration can serve as a field variable which differs between a Li-rich and a Li-poor phase separated by a diffuse interface.

(i) Li-interacalation: The thermodynamics of phase separation can be systematically described by phase field models [4, 8, 18, 21, 36] which rely on a thermodynamic free energy functional

$$F_r(c_s) = n_v \int_{D_s} f_r(c_s) + \tilde{\lambda}(\nabla c_s)^2 \, d\mathbf{x}, \tag{2.1}$$

where f is the homogeneous free energy of a regular solution, that is,

$$f_r(c_s) = \omega c_s(1-c_s) + k_B T\left(c_s \log c_s + (1-c_s)\log(1-c_s)\right). \tag{2.2}$$

The parameter ω in (2.2) is an effective interaction energy between a Li interstitial site and its neighbouring (Li-free) sites. The parameter λ, which accounts for the strength of penalisation of concentration gradients, is proportional to the interfacial width and assumes in the case of $LiFePO_4$ as intercalation material the following form,

$$\tilde{\lambda} = a^2\omega/6, \tag{2.3}$$

where ω =59meV is the nearest neighbour interaction energy and $a = 2.5\mathring{A}$ the nearest neighbour distance. Using also $n_v = 8.396 \times 10^{28}[/m^3]$ then leads to $\lambda = n_v\tilde{\lambda} = 2.48 \times 10^{-11} J/m$ as in [21].

Taking a mass conserving gradient flow, i.e., computing the variational derivative with respect to test functions $v \in H^1(D_s)$, we obtain up to boundary terms

$$\partial_t c_s = -\mathrm{div}\left(\hat{\mathrm{M}}\nabla\left(\nabla_{c_s}^{H^1} F_r(c_s)\right)\right), \tag{2.4}$$

where the derivative $\nabla_c^{H^1}$ represents the Gâteaux derivative. That means, for all $v \in H^1(D_s)$ we compute

$$\frac{\delta^v F_r(c_s)}{\delta^v c_s} = \lim_{\theta\to 0}\frac{F_r(c_s+\theta v) - F_r(c_s)}{\theta} = ((f_r'(c_s) - \lambda\Delta c_s), v) = \left(\nabla_{c_s}^{L^2} F_r(c_s), v\right), \tag{2.5}$$

where the last equality identifies $\nabla_{c_s}^{L^2} F_r(c_s)$ by Riesz's theorem. In the same way we can apply Riesz's theorem with respect to the semi-inner product $\left(\hat{\mathrm{M}}\nabla u, \nabla v\right)_{H^1}$ for $u, v \in H^1(D_s)$ and a

symmetric positive definite tensor $\hat{\mathrm{M}}$ to define $\nabla_{c_s}^{H^1} F_r(c_s)$ under homogeneous Neumann boundary conditions as follows

$$\left(\nabla_{c_s}^{H^1} F_r(c_s), v\right) = \left(\hat{\mathrm{M}}\nabla\nabla_{c_s}^{L^2} F_r(c_s), \nabla v\right) = \left(-\mathrm{div}\left(\hat{\mathrm{M}}\nabla_{c_s}^{L^2} F_r(c_s)\right), v\right). \tag{2.6}$$

Putting (2.12)–(2.6) together, leads with $f_r'(c_s) = \omega(1-2c_s) + k_B T \log\left(\frac{c_s}{1-c_s}\right)$ to the phase field equation for intercalation compounds

$$\partial_t c_s = \mathrm{div}\left(\hat{\mathrm{M}}\nabla\left(f_r'(c_s) - \lambda\Delta c_s\right)\right), \tag{2.7}$$

where the mobility tensor $\hat{\mathrm{M}}$ is often chosen as a constant M_s since generally it is difficult to trace back the irreversible behaviour to the underlying frictional processes after coarse graining. A state equation with concentration dependent mobility is suggested in [21], i.e., $\hat{\mathrm{M}} = c_s(1-c_s)M_0$ where M_0 is a constant.

(ii) Electron transport: We describe charge transport in the solid matrix by the current

$$i_s = -\sigma_s \nabla \psi_s, \tag{2.8}$$

where σ_s is the conductivity of the solid intercalation phase D_s and ψ_s is the electric potential in D_s. Equation (2.8) is widely used in the literature, e.g. [48].

(E) Electrolyte/separator:
A large part of the electrochemical literature is dedicated to transport equations for binary electrolytes. These denote solutions containing a single binary salt of the form $\mathrm{X_1X_2}$ plus a solvent (generally polymer in Li-batteries) where $\mathrm{X_1^+}$ and $\mathrm{X_2^-}$ represent a cation and an anion, respectively. Electrolytes $\mathrm{X_1X_2}$ that dissociate into an equal number of cations ν_+ and anions ν_- are called *symmetric*. Subsequently, we present four different formulations **(E1)**–**(E4)** for binary electrolytes.

(E1) *Dilute solution theory: charge transport by Poisson-Nernst-Planck (PNP).* There is a wide range of different modelling approaches as well as analytical studies of charge transport formulations such as [17, 24, 27, 29, 40, 41, 45]. Recently, the PNP system has been modified to describe electrolytes beyond the dilute approximation in [15], see also Remark 2.1 below. The widely used and well-accepted Nernst-Planck formulation allows us to take the densities c_i of each species i in the solution into account. Since we consider a polymer electrolyte as a solution, we have a neutral ($z_0 = 0$) density c_0 for the polymer solvent, the cation density $c_+ = c_1$ of lithium ions $\mathrm{X_1^+}$, and the anion density $c_- = c_2$ of negative salt ion $\mathrm{X_2^-}$. The following classical and well-accepted description is based on the PNP system,

$$\text{(PNP)} \qquad \begin{cases} \partial_t c_i + \mathbf{u}\cdot\nabla c_i = \mathrm{div}\left(D_i\nabla c_i + e z_i c_i M_i \nabla\psi\right), & \text{for } i = 0,1,2, \\ -\mathrm{div}\left(\varepsilon\nabla\psi\right) = e\sum_{i=0}^{2} z_i c_i, \end{cases} \tag{2.9}$$

where M_i, D_i, and z_i are the diffusion, mobility, and charge number of species i, respectively. The parameter ε is the electric permittivity of the electrolyte and e denotes the elementary charge. The fluid velocity $\mathbf{u}$ is the solution of the incompressible Navier-Stokes (iNS) equations extended by a Coulomb force term on the right-hand side [24, 40, 41], i.e.,

$$\text{(iNS)} \qquad \begin{cases} \partial_t \mathbf{u} + \mathbf{u}\cdot\nabla\mathbf{u} - \Delta\mathbf{u} + \nabla p = -e\sum_{i=0}^{2} z_i c_i \nabla\psi, \\ \mathrm{div}\,\mathbf{u} = 0. \end{cases} \tag{2.10}$$

In the context of the dilute solution theory, see Remark 2.1 below for more details, one does not use the flux of the solvent, i.e., $i=0$ in (2.9), but instead the solvent is solely described by the momentum equation (2.10). For simplicity, we will subsequently denote the cation density by c_+, the anion density by c_-.

(E2) *Binary electrolyte [48].* Since bulk *electroneutrality* is a widely confirmed characteristic property of solutions, we make the frequent assumption of an electrically neutral solution, i.e.,

$$\sum_i z_i c_i = 0\,. \tag{2.11}$$

We note that the neutrality assumption (2.11) is violated in interfacial regions (e.g. near electrodes) where thin *electrical double layers (EDL)* appear. Under electroneutrality, the concentration of the electrolyte is consistently defined by

$$c := \frac{c_+}{\nu_+} = \frac{c_-}{\nu_-}\,. \tag{2.12}$$

Moreover, we assume constant mobilities and diffusion coefficients. Applying the fluxes $\mathbf{j}_i$, $i=1,2$, from the Nernst-Planck setting (2.9) leads to

$$\begin{cases} \partial_t c + \mathbf{u}\cdot\nabla c = D\Delta c, \\ (z_+M_+ - z_-M_-)F\operatorname{div}(c\nabla\psi) + (D_+ - D_-)\Delta c = 0, \end{cases} \tag{2.13}$$

where $D = \frac{z_+M_+D_- - z_-M_-D_+}{z_+M_+ - z_-M_-}$.

Remark 2.1 (Validity) *The dilute solution theory is recommended as a general formulation since it is widely used in the electrochemical literature and at the same time it accounts for the essential physical processes involved without very complicated/less accessible ingredients [48, p.274]. But one should be aware that the fluxes defined in* $(2.9)_1$ *break down because electro-migration and diffusion are not consistently defined with respect to an average velocity* $\mathbf{u}$ *of the fluid. A way out of this is a so-called* dilute solution *where one does not apply (2.9) to the solvent, i.e.,* $i=0$*, but solely to the ionic species and where one attributes the fluid velocity* $\mathbf{u}$ *to the velocity of the solvent.*

Recently, the authors of [15] have carefully specified the fluid velocity $\mathbf{u}$ *in order to overcome the above noted difficulty.* ◇

(E3) *Concentrated solution.* We state a charge transport model for a polymer electrolyte as proposed in [14] for composite cathodes. This transport formulation relies on experimentally measurable quantities such as the transference number. We still assume that the polymer electrolyte is a solution of a binary salt and a solvent. For a Li-polymer insertion cell the solution is for instance a binary salt LiX and the solvent a polymer. Taking the polymer as a reference species, the following material balance on the lithium salt electrolyte $c=c_i/\nu_i$,

$$\partial_t c = \operatorname{div}\left(D(c)\left(1 - \frac{d(\ln c_0)}{d(\ln c)}\right)\nabla c\right) - \frac{\mathbf{i}_p\cdot\nabla t_+^0(c)}{z_+\nu_+F}\,, \tag{2.14}$$

where $t_j = \frac{z_j^2M_jc_j}{\sum_i z_i^2M_ic_i}$ is the experimentally obtained transference number which accounts for the current associated with species j. In [14], the following fit to experimental data is employed

$$t_+^0 = 0.0107907 + 1.48837\times10^{-4}c. \tag{2.15}$$

Following again the concentrated solution theory [48] applied to lithium-polymer insertion cells in [14], the current $\mathbf{i}_p$ in the polymer phase admits the following representation

$$\mathbf{i}_p := -\kappa(c)\nabla\psi_p - \frac{\kappa(c)RT}{F}\left(1+\frac{\partial \ln f_\pm}{\partial \ln c}\right)\left(\frac{s_+}{n\nu_+}+\frac{t_+^0(c)}{z_+\nu_+}\right)\nabla \ln c, \tag{2.16}$$

where the electric potential ψ_p in the polymer phase is measured with a reference electrode, $\kappa = F\sum_i z_i^2 M_i c_i$ is the conductivity of the solution not accounting for concentration gradients. The variable $f_\pm$ is the activity coefficient of the salt and is only accounted for if data are available [14].

(E4) *Onsager-type equations away from equilibrium.* The subsequent charge transport formulation has been introduced in [16]. The concentration of lithium c^+ in the electrolyte phase is governed by the following system

$$\begin{aligned} \partial_t c^+ &= \operatorname{div}\left(k_{11}^+(c^+)\nabla c^+ + k_{12}^+\nabla\psi\right) = 0, \\ 0 &= \operatorname{div}\left(k_{21}^+(c^+)\nabla c^+ + k_{22}^+\nabla\psi\right), \end{aligned} \tag{2.17}$$

where the coefficients are defined for the ion conductivity κ^+ and ion diffusion coefficient D^+ by

$$\begin{aligned} k_{11}^+(c^+) &= D^+ + \frac{RT}{F^2}\frac{(t_+)^2\kappa^+}{c^+}, \qquad k_{12}^+ = \kappa^+\frac{t_+}{F}, \\ k_{21}^+(c^+) &= \frac{RT}{F}\frac{\kappa^+ t_+}{c^+}, \qquad k_{22}^+ = \kappa^+. \end{aligned} \tag{2.18}$$

Remark 2.2 (Comments to formulations **(E1)**–**(E4)**) *The formulations* **(E1)**-**(E2)** *are widely used in theory and computational modelling whereas* **(E3)** *is generally used in experimental science in view of particular parameters that represent directly measurable quantities. The transport equations* **(E4)** *are interesting as they resemble in their stationary form the classical Onsager relations [34, 35].* ◇

(I) Solid-electrolyte interphase:
The interfacial transition of Li from the polymer solution into the solid insertion compound is governed by the Butler-Volmer kinetics [3, 5]. Following Doyle et al. [14], the following reaction

$$\mathrm{Li}^+ - \Theta_p + \Theta_s + e^- \quad \rightleftharpoons \quad \mathrm{Li} - \Theta_s + \Theta_p, \tag{2.19}$$

governs the Li insertion into the solid matrix. The variables Θ_p and Θ_s stand for the available sites in the polymer and the solid matrix (interstitial). For an overpotential $\eta := \psi_s - \psi$ between the solid (ψ_s) and the bulk electrolyte (ψ) and the voltage $U = U_2^\theta - U_{\mathrm{ref}}^\theta + RT/F(\beta c_s + \zeta)$, the insertion process (2.19) induces the current

$$i = Fk_{\mathrm{fb}}(c_{\mathrm{pm}} - c)^{\alpha_c} c^{\alpha_a}\left[c_s \exp\left(\frac{\alpha_a F}{RT}(\eta - U)\right) - (c_{\mathrm{sm}} - c_s)\exp\left(-\frac{\alpha_c F}{RT}(\eta - U)\right)\right], \tag{2.20}$$

where c_{sm} and c_{pm} are the maximal densities in the solid and the polymer phase, respectively. The variable ζ is a constant expressing corrections to activity. We will set these parameters according to [14], i.e., $c_{\mathrm{sm}} = 29000\mathrm{mol/m^3}$, $c_{\mathrm{pm}} = 3920\mathrm{mol/m^3}$. Additionally, the transfer coefficients are $\alpha_a = \alpha_c 0.5$, and the reaction rate at the particle-electrolyte interface is $k_{\mathrm{fb}} = 10^{-10}\mathrm{m^4/(mol\cdot s)}$.

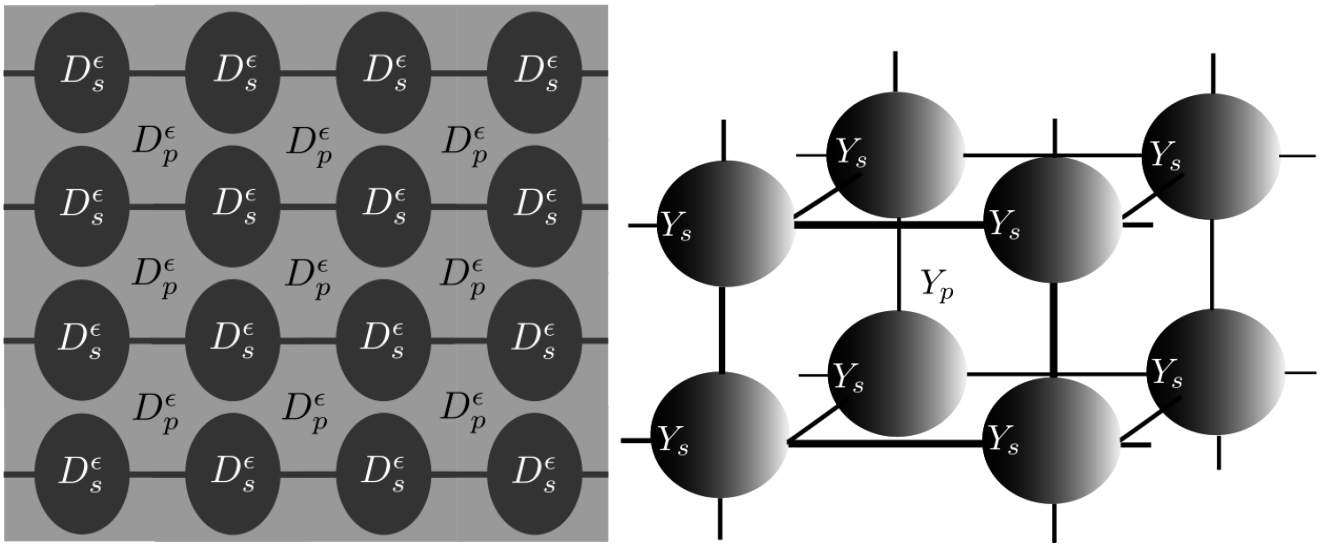

Figure 2: **Left:** A 2D periodic composite cathode $D = D_p^\epsilon \cup D_s^\epsilon$ of characteristic length L with solid intercalation particles D_s^ϵ surrounded by a polymer electrolyte solution. This black lines are electric conducting pathways in the form carbon black. This cell motivates a layer by layer assembly. We note that this figure can serve as a reference cell that represents a characteristic configuration of intercalation particles electrically connected in various ways via carbon black, and surrounded by polymer electrolyte. **Right:** A 3D sample reference cell of a possible cathode composed of $FePO_4$ particles connected via carbon black particles (thin lines). Obviously, more complex cells can be used.

Hence, the intercalation current density (2.20) governs how the the Li^+-flux $\mathbf{j}_p = \hat{M}_p \nabla (c + z_+ c \nabla \psi_p)$ from the polymer solution is related to the Li-flux $\mathbf{j}_s = \hat{M}_s \nabla (f'(c_s) - \lambda \Delta c_s)$ in the solid intercalation compound. Based on the interfacial reaction (2.19), we have the following boundary conditions on the interface,

$$\text{(Interfacial kinetics)} \qquad \begin{cases} i = -\frac{s_i}{nF} \mathbf{j}_p \cdot \mathbf{n} & \text{on } \partial D_p, \\ i = -\mathbf{j}_s \cdot \mathbf{n} & \text{on } \partial D_s, \\ i = -\sigma_s \nabla \phi_s & \text{on } \partial D_s, \end{cases} \tag{2.21}$$

where $\mathbf{n}$ is the outward normal of the corresponding domains and the number of electrons is one, that is, $n = 1 = s_i$, where s_i is the stochiometric parameter.

2.2 Microscopic equations for composite cathodes

Based on the previous Section 2.1, we can now state the microscopic system of equations describing charge transport in a periodically extended composite cathode, see Fig. 2. We distinguish two different microscales, that is, a reference pore scale of characteristic length l_p and a so-called Darcy scale of characteristic length l_D. Herewith, mass transport is governed by the heterogeneity $\epsilon_p = \frac{l_p}{L}$ of pores where l_p is the characteristic size of a reference particle configuration and L is the macroscopic length of the composite cathode. The microscopic formulation fully resolves the highly heterogeneous geometry of the composite cathode in which we have to account for three essential transport mechanisms: (1) Diffusive and electro-migrational transport in the polymer

solution

$$D_p^{\epsilon_p} := \bigcup_{\mathbf{z}\in\mathbb{Z}^d} \epsilon_p (Y_p + \mathbf{z}) \cap D;$$

(2) Interstitial diffusion inside a solid intercalation compound

$$D_s^{\epsilon_p} := \bigcup_{\mathbf{z}\in\mathbb{Z}^d} \epsilon_p (Y_s + \mathbf{z}) \cap D$$

(described by a mean field phase field equation); and (3) Reaction kinetics on the interface $I^{\epsilon_p} := \partial D_p^{\epsilon_p} \cap \partial D_s^{\epsilon_p}$ given by the Butler-Volmer equations (2.20) which are imposed as boundary conditions.

The following equations fully describe the microscopic kinetic processes in the composite cathode and hence are indexed by the pore heterogeneity ϵ_p. Moreover, we allow for a further length scale $l_D > l_p$, called Darcy scale, see Fig. 1 **Right**. This then leads to a so-called Darcy's heterogeneity $\epsilon_D := \frac{l_D}{L}$. We note that the subsequent results are valid for scenarios where the pore scale ϵ_p differs from the Darcy scale ϵ_D, i.e., where $\epsilon_p < \epsilon_D$. Hence, the scaling $\epsilon_p < \epsilon_D$ enables us to account for a third scale via the momentum equation. Hence, fluid flow is considered on a perforated domain

$$D_p^{\epsilon_D} := \bigcup_{\mathbf{z}\in\mathbb{Z}^d} \epsilon_D (Y_D^p + \mathbf{z}) \cap D$$

which is defined by a slightly larger representative volume element Y_D^p accounting for the Darcy scale l_D. As the boundary conditions on ∂D do not have a direct influence in the upscaling inside the composite cathode D, we do not state here how D interacts with external forces and systems as this can still be made precise at a later stage.

Due to confined material structure, one can expect a fast relaxation time for the flow as well as a small characteristic flow field. Therefore, the flow is governed by a small Reynolds number $Re = \frac{\rho U_{ref} L}{\mu}$ (where ρ is the density of the fluid, U_{ref} is a reference velocity, μ the dynamic viscosity, and L a characteristic length of the system) and hence instead of using the full time-dependent Navier-Stokes equations to define $\mathbf{u}^{\epsilon_D}$, we can apply a quasi-stationary formulation based on Stokes equations, i.e.,

$$\begin{cases} -\epsilon_D^2 \mu \Delta \mathbf{u}^{\epsilon_D} + \nabla p^{\epsilon_D} = \mathbf{f}^{\epsilon_p} := -e(z_+ c_+^{\epsilon_p} - z_- c_-^{\epsilon_p}) \nabla \psi_p^{\epsilon_p} & \text{in } D_p^{\epsilon_D}, \\ \operatorname{div} \mathbf{u}^{\epsilon_D} = 0 & \text{in } D_p^{\epsilon_D}, \end{cases} \tag{2.22}$$

where $-e(z_+ c_+^{\epsilon_p} - z_- c_-^{\epsilon_p}) \nabla \psi_p^{\epsilon_p}$ is a Coulomb driving force [24, 40, 41]. In the polymer electrolyte (binder), we have

$$\begin{cases} \partial_t c_+^{\epsilon_p} + \mathbf{u}^{\epsilon_p} \cdot \nabla c_+^{\epsilon_p} = \operatorname{div}\left(k_B T M_+ \left(\nabla c_+^{\epsilon_p} + e z_+ c_+^{\epsilon_p} \nabla \psi_p^{\epsilon_p}\right)\right) & \text{in } D_p^{\epsilon_p}, \\ \partial_t c_-^{\epsilon_p} + \mathbf{u}^{\epsilon_p} \cdot \nabla c_-^{\epsilon_p} = \operatorname{div}\left(k_B T M_- \left(\nabla c_-^{\epsilon_p} - e z_- c_-^{\epsilon_p} \nabla \psi_p^{\epsilon_p}\right)\right) & \text{in } D_p^{\epsilon_p}, \\ -\operatorname{div}\left(\varepsilon_p \nabla \psi_p^{\epsilon_p}\right) = e(z_+ c_+^{\epsilon_p} - z_- c_-^{\epsilon_p}) & \text{in } D_p^{\epsilon_p}, \end{cases} \tag{2.23}$$

where the parameter ε_p denotes the electric permittivity of the polymer and hence differs from the pore heterogeneity ϵ_p. The variable $c = c_+$ denotes the density of Li^+-ions. The mean field equations describing interstitial and electron transport inside a solid crystal read in the pore scale as follows

$$\begin{cases} \partial_t c_s^{\epsilon_p} = \operatorname{div}\left(M_s \nabla \left(f_r'(c_s^{\epsilon_p}) - \lambda \Delta c_s^{\epsilon_p}\right)\right) & \text{in } D_s^{\epsilon_p}, \\ -\operatorname{div}\left(\sigma_s \nabla \phi_s^{\epsilon_p}\right) = 0 & \text{in } D_s^{\epsilon_p}, \end{cases} \tag{2.24}$$

where the electric conductivity of the solid intercalation compound is σ_s. We note that the Poisson equations $(2.33)_3$ and $(2.24)_2$ can be written as a single equation for the electric potential ϕ^{ϵ_p} by

$$-\mathrm{div}\,(\varepsilon(\mathbf{x}/\epsilon_p)\nabla\psi^{\epsilon_p}) = e(z_+c_+^{\epsilon_p} + z_-c_-^{\epsilon_p})\chi_{D_p^{\epsilon_p}} \qquad \text{in } D, \tag{2.25}$$

valid on the whole domain D for the combined permeability and conductivity parameter

$$\varepsilon(\mathbf{x}/\epsilon) := \varepsilon_p\chi_{Y_p}(\mathbf{x}/\epsilon_p) + \sigma_s\chi_{Y_s}(\mathbf{x}/\epsilon_p), \tag{2.26}$$

and with the characteristic function $\chi_{D_p^{\epsilon_p}}(\mathbf{x}) = 1$ if $\mathbf{x}\in D_p^{\epsilon_p}$. In (2.26), we employ the microscopic variable $\mathbf{y}\in Y$ defined on the reference cell Y, see Fig. 1 for a sample polymer-particle configuration of a composite cathode.

In order to complete the microscopic formulation, we still need to state the interfacial processes taking place on the polymer/binder-solid interface I^{ϵ_p}, i.e.,

$$\begin{cases} \epsilon_p R^{\epsilon_p}(c_+^{\epsilon_p}, c_s^{\epsilon_p}, \eta^{\epsilon_p}, U^{\epsilon_p}) = \frac{RT}{F}\left(M_+\left(\nabla c_+^{\epsilon_p} + ez_+c_+^{\epsilon_p}\nabla\psi^{\epsilon_p}\right) - \mathbf{u}^{\epsilon_D}c_+^{\epsilon_p}\right)\cdot\mathbf{n}_{ps} & \text{on } I^{\epsilon_p}, \\ 0 = \frac{RT}{F}\left(M_-\left(\nabla c_-^{\epsilon_p} - ez_-c_-^{\epsilon_p}\nabla\psi^{\epsilon_p}\right) - \mathbf{u}^{\epsilon_D}c_-^{\epsilon_p}\right)\cdot\mathbf{n}_{ps} & \text{on } I^{\epsilon_p}, \\ \epsilon_p R^{\epsilon}(c_+^{\epsilon_p}, c_s^{\epsilon_p}, \eta^{\epsilon_p}, U^{\epsilon_p}) = -M_s\nabla\left(f_r'(c_s^{\epsilon_p}) - \lambda\Delta c_s^{\epsilon_p}\right)\cdot\mathbf{n}_{sp} & \text{on } I^{\epsilon_p}, \\ \epsilon_p R^{\epsilon_p}(c^{\epsilon_p}, c_s^{\epsilon_p}, \eta^{\epsilon_p}, U^{\epsilon_p}) = \sigma_s\nabla\psi_s^{\epsilon}\cdot\mathbf{n}_{sp} & \text{on } I^{\epsilon_p}, \\ \sigma_s\nabla\psi_p^{\epsilon_p}\cdot\mathbf{n}_{sp} = \varepsilon_p\nabla\psi_s^{\epsilon_p}\cdot\mathbf{n}_{sp} & \text{on } I^{\epsilon_p}, \\ \mathbf{u}^{\epsilon_D} = \mathbf{0} & \text{on } I^{\epsilon_p}, \end{cases} \tag{2.27}$$

where $\mathbf{n}_{sp} = -\mathbf{n}_{ps}$ are normals pointing outward from the solid into the polymer or from the polymer into the solid phase, respectively. The current $R^{\epsilon_p} = R^{\epsilon_p}(c^{\epsilon_p}, c_s^{\epsilon_p}, \eta^{\epsilon_p}, U^{\epsilon_p})$ is defined by the Butler-Volmer kinetics (2.20) extended here towards the highly heterogeneous composite cathode setting indicated by the pore heterogeneity ϵ_p, that is,

$$R^{\epsilon_p} = i_{ps}\left[\frac{c_s^{\epsilon_p}}{c_{sm}^{\epsilon_p}}\exp\left(\alpha_{sm}\frac{\alpha_a F}{RT}(\eta^{\epsilon_p} - U^{\epsilon_p})\right) - \frac{(c_{\mathrm{sm}}^{\epsilon_p} - c_s^{\epsilon_p})}{c_{sm}^{\epsilon_p}}\exp\left(-\alpha_{sm}\frac{\alpha_c F}{RT}(\eta^{\epsilon_p} - U^{\epsilon_p})\right)\right], \tag{2.28}$$

where $i_{ps} = Fk_{\mathrm{fb}}(c_{\mathrm{pm}}^{\epsilon_p} - c^{\epsilon_p})^{\alpha_c}(c^{\epsilon_p})^{\alpha_a}$ plays the role of an exchange current density and $c_{sm}^{\epsilon_p} = \exp(\alpha_{sm})$ brings the term in the angled brackets into dimensionless form. For the limits $\lim_{\mathbf{x}\to I_s^{\epsilon_p}}$ and $\lim_{\mathbf{x}\to I_p^{\epsilon_p}}$, which denote passing from the solid phase and the polymer phase to the interface I^{ϵ_p}, respectively, we can identify the overpotential in (2.28) by

$$\eta^{\epsilon_p} = \lim_{\mathbf{x}\to I_s^{\epsilon_p}}\psi^{\epsilon_p} - \lim_{\mathbf{x}\to I_p^{\epsilon_p}}\psi^{\epsilon_p}. \tag{2.29}$$

Equation (2.28) additionally depends on the maximum capacity of ions in the polymer phase $c_{\mathrm{pm}}^{\epsilon_p} = 3920\mathrm{mol/m^3}$ as well as in the solid crystal $c_{\mathrm{sm}}^{\epsilon_p} = 29000\mathrm{mol/m^3}$. We also recall from equation (2.20) that a fitting to experimental data [14, 50] provides

$$U^{\epsilon_p} = 2.17 + \frac{RT}{F}\left(-0.000558\,c_s^{\epsilon_p}\big|_{I^{\epsilon_p}} + 8.1\right). \tag{2.30}$$

Finally, we bring the equations (2.22), (2.24), (2.25), and (2.27) into *dimensionless form* by using the following variables and parameters

$$\begin{gathered} \tilde{\mathbf{u}}^{\epsilon_D} = \frac{\mathbf{u}^{\epsilon_D}}{U_{\mathrm{ref}}}, \quad \tilde{c}_{\pm}^{\epsilon_p} = \frac{c_{\pm}^{\epsilon_p}}{c_{\mathrm{ref}}}, \quad \tilde{\psi} = \frac{F\psi}{RT}, \quad \tilde{t} = \frac{t}{\tau}, \\ \tilde{\mathbf{x}} = \frac{\mathbf{x}}{L}, \quad \eta = \frac{2c_{\mathrm{ref}}RTL}{U_{\mathrm{ref}}\mu}, \quad Pe = \frac{LU_{\mathrm{ref}}}{D}, \end{gathered} \tag{2.31}$$

where τ is either the diffusion time $\tau_D := \frac{L^2}{D}$, the interfacial transport time $\tau_s := \frac{L^2}{M_s}$, or the convection time $\tau_u = \frac{L}{U_{ref}}$. U_{ref} is a reference velocity and c_{ref} a reference salt concentration. We also use the identity $\frac{k_B T}{e} = \frac{RT}{F}$ and the electric potential ψ stands for the electric potentials of the solid phase ψ_s and of the liquid phase ψ_p. The parameter $\lambda_D := \left(\frac{\epsilon_p k_B T}{2e^2 c_{\text{ref}}}\right)^{1/2}$ denotes the dimensionless Debye length and $\sigma := \frac{\sigma_s}{\sigma_{\text{ref}}}$ the dimensionless electric conductivity. We set the reference conductivity to the bulk conductivity in the electrolyte phase, i.e., $\sigma_{ref} = \frac{\varepsilon_p D}{\lambda^2}$. For notational convenience, we assume $M = M_+ = M_-$, and hence $D = D_+ = D_-$, and we will subsequently drop the tilde from dimensionless variables. With Einstein's relation we then have $D = k_B T M$. Moreover, we note that the convection-diffusion-electromigration equation reads with the above scalings as follows

$$\frac{L^2}{\tau D}\frac{\partial \tilde{c}_\pm^{\epsilon_p}}{\partial \tilde{t}} + Pe\,\tilde{\mathbf{u}}^{\epsilon_D}\tilde{\nabla}\tilde{c}_\pm^{\epsilon_p} = \tilde{\text{div}}\left(z_\pm \tilde{c}_\pm^{\epsilon_p}\tilde{\nabla}\tilde{\psi}\right).$$

As noted earlier in this section, in the composite cathode one expects a small $Re = Pe/\text{Pr}$ but a large Prandtl number $\text{Pr} := \frac{\nu}{D}$, e.g. in solute transport in groundwater flow $D = 10^{-5} cm^2/s$, $\nu = 10^{-2} cm^2/s$, and hence $\text{Pr} = 10^3$, where $\nu = \frac{\mu}{\rho}$ is the the kinematic viscosity and ρ the density. Therefore, we allow for $Pe = \mathcal{O}(1)$ [31].

Herewith and after choosing $\tau = \tau_u$, and setting $\frac{\tau_s}{\tau_u} = 1$ for simplicity, we obtain the following dimensionless microscopic formulation

$$\text{(micro } \textbf{(SE)}\text{)} \qquad \begin{cases} -\epsilon_D^2 \Delta \mathbf{u}^{\epsilon_D} + \nabla p^{\epsilon_D} = \mathbf{f}^{\epsilon_p} := -\eta(z_+ c_+^{\epsilon_p} - z_- c_-^{\epsilon_p})\nabla\psi^{\epsilon_p} & \text{in } D_p^{\epsilon_D}, \\ \text{div}\,\mathbf{u}^{\epsilon_D} = 0 & \text{in } D_p^{\epsilon_D}. \end{cases} \tag{2.32}$$

$$\text{(micro } \textbf{(E1)}\text{)} \qquad \begin{cases} Pe\left(\partial_t c_+^{\epsilon_p} + \mathbf{u}^{\epsilon_p}\cdot\nabla c_+^{\epsilon_p}\right) = \text{div}\left(\nabla c_+^{\epsilon_p} + z_+ c_+^{\epsilon_p}\nabla\psi^{\epsilon_p}\right) & \text{in } D_p^{\epsilon_p}, \\ Pe\left(\partial_t c_-^{\epsilon_p} + \mathbf{u}^{\epsilon_p}\cdot\nabla c_-^{\epsilon_p}\right) = \text{div}\left(\nabla c_-^{\epsilon_p} - z_- c_-^{\epsilon_p}\nabla\psi^{\epsilon_p}\right) & \text{in } D_p^{\epsilon_p}, \end{cases} \tag{2.33}$$

$$\text{(micro } \textbf{(S)}\text{)} \qquad \left\{ \partial_t c_s^{\epsilon_p} = \text{div}\left(\nabla\left(f_r'(c_s^{\epsilon_p}) - \lambda\Delta c_s^{\epsilon_p}\right)\right) \right. \qquad \text{in } D_s^{\epsilon_p}, \tag{2.34}$$

$$\text{(micro } \textbf{(P)}\text{)} \qquad \begin{cases} -\text{div}\left(\lambda_D\nabla\psi_p^{\epsilon_p}\right) = (z_+ c_+^{\epsilon_p} + z_- c_-^{\epsilon_p}) & \text{in } D_p^{\epsilon_p}, \\ -\text{div}\left(\sigma\nabla\psi_s^{\epsilon_p}\right) = 0 & \text{in } D_s^{\epsilon_p}, \end{cases} \tag{2.35}$$

$$\text{(micro } \textbf{(I)}\text{)} \qquad \begin{cases} \epsilon_p\beta_+ R^{\epsilon_p}(c_+^{\epsilon_p}, c_s^{\epsilon_p}, \eta^{\epsilon_p}, U^{\epsilon_p}) = \left(\left(\nabla c_+^{\epsilon_p} + z_+ c_+^{\epsilon_p}\nabla\psi^{\epsilon_p}\right) - \mathbf{u}^{\epsilon_D} c_+^{\epsilon_p}\right)\cdot\mathbf{n}_{ps} & \text{on } I^{\epsilon_p}, \\ 0 = \left(\left(\nabla c_-^{\epsilon_p} - z_- c_-^{\epsilon_p}\nabla\psi^{\epsilon_p}\right) - \mathbf{u}^{\epsilon_D} c_-^{\epsilon_p}\right)\cdot\mathbf{n}_{ps} & \text{on } I^{\epsilon_p}, \\ \epsilon_p\beta_s R^{\epsilon}(c_+^{\epsilon_p}, c_s^{\epsilon_p}, \eta^{\epsilon_p}, U^{\epsilon_p}) = -\nabla\left(f_r'(c_s^{\epsilon_p}) - \lambda\Delta c_s^{\epsilon_p}\right)\cdot\mathbf{n}_{sp} & \text{on } I^{\epsilon_p}, \\ \epsilon_p\beta_\psi R^{\epsilon_p}(c_+^{\epsilon_p}, c_s^{\epsilon_p}, \eta^{\epsilon_p}, U^{\epsilon_p}) = \sigma\nabla\psi_s^{\epsilon}\cdot\mathbf{n}_{sp} & \text{on } I^{\epsilon_p}, \\ \frac{\sigma_s}{\sigma_{ref}}\nabla\psi_p^{\epsilon_p}\cdot\mathbf{n}_{sp} = \frac{\varepsilon_p}{\varepsilon_s}\nabla\psi_s^{\epsilon_p}\cdot\mathbf{n}_{sp} & \text{on } I^{\epsilon_p}, \\ \mathbf{u}^{\epsilon_D} = \mathbf{0} & \text{on } I^{\epsilon_p}. \end{cases} \tag{2.36}$$

where the parameters coupling the Butler-Volmer reactions to the different charge transport equations are defined by $\beta_+ = \frac{i_{ps}L}{eD}, \beta_s = \frac{i_{ps}L}{eM},$ and $\beta_\psi = \frac{F}{RT}\frac{i_{ps}L}{\sigma_{ref}}$ for $\sigma_{ref} = \frac{\varepsilon_p D}{\lambda_D^2}$.

A summary of physical and dimensionless parameters are given in Tab. 2.

3 Main results: Effective macroscopic equations

Our main result is the reliable and systematic derivation of a novel set of effective macroscopic composite cathode equations that take the crucial chemical and transport processes described in Section 2.2 into account: (a) ionic transport; (b) interfacial reactions; (c) intercalation dynamics under a possible phase transformation; (d) electron transport.

The subsequent upscaling result relies on the following property.

Definition 3.1 (Local Thermodynamic Equilibrium (LTE)) *The chemical potentials* $\mu_\pm(C^\pm,\Psi)=\log C^\pm\pm\Psi$ *and* $\mu_s(C_s)=f_r'(C_s)-\frac{\lambda}{q}\mathrm{div}\left(\hat{\mathbb{M}}\nabla C_s\right)$ *are said to be in local thermodynamic equilibrium if for every* $k\in\mathbb{N}$, $1\le k\le d$,

$$\frac{\partial\mu_\iota(C^\iota,\Psi)}{\partial x_k}=\begin{cases}0 & \text{if it appears in the cell problem in } Y\times D,\\ \frac{\partial\mu^\iota(C^\iota,\Psi)}{\partial x_k} & \text{if it appears on the macroscale } D,\end{cases}\tag{3.37}$$

and similarly

$$\frac{\partial\mu_s(C^s)}{\partial x_k}=\begin{cases}0 & \text{if it appears in the cell problem in } Y\times D,\\ \frac{\partial\mu_s(C^s)}{\partial x_k} & \text{if it appears on the macroscale } D,\end{cases}\tag{3.38}$$

for $\iota=+,-$, *where* $C^\pm$, Ψ, *and* C^s *are the upscaled/slow variables solving (3.39) below and do not depend on the fast microscale* Y.

With the help of the asymptotic two-scale expansion method, we derive the following

Main result: (Upscaled composite cathode equations) *The microscopic composite cathode formulation based on the equations (2.32), (2.33), (2.34), and (2.36) admits under local thermodynamic equilibrium (Definition 3.1) the following upscaled/homogenized equations*

$$\begin{cases}
\mathbf{V}(\mathbf{x},t)=-\frac{\hat\kappa}{\mu}(\mathbf{f}^0-\nabla P) & \text{in } D,\\
\quad\mathrm{div}\,\mathbf{V}=0, & \text{in } D,\\
p\partial_t C^+ + Pe\mathbf{V}\cdot\nabla C^+=\mathrm{div}\left(\hat{\mathbb{D}}\nabla C^+ + z_+C^+\hat{\mathbb{M}}\nabla\Psi_p\right)-\overline{\beta}_+R(C^+,C^s,\eta^0,U^0) & \text{in } D,\\
p\partial_t C^- + Pe\mathbf{V}\cdot\nabla C^-=\mathrm{div}\left(\hat{\mathbb{D}}\nabla C^- - z_-C^-\hat{\mathbb{M}}\nabla\Psi_p\right) & \text{in } D,\\
-\mathrm{div}\,(\hat\varepsilon\nabla\Psi_p)=p(z_+C^+ + z_-C^-) & \text{in } D,\\
-\mathrm{div}\left(\hat\Sigma\nabla\Psi_s\right)=\overline{\beta}_\psi R(C^+,C^s,\eta^0,U^0) & \text{in } D,\\
q\partial_t C_s=\mathrm{div}\left(\hat{\mathbb{M}}_s\left(\nabla f_r'(C_s)+\frac{\lambda}{q}\mathrm{div}\left(\hat{\mathbb{M}}_s\nabla C_s\right)\right)\right)+\overline{\beta}_s R(C_+,C_s,\eta^0,U^0) & \text{in } D,
\end{cases}\tag{3.39}$$

where $p=\frac{|Y_1|}{|Y|}$, $q=1-p$, $\mathbf{f}^0=-\eta(C_+-C_-)\hat{\mathbb{M}}\nabla\Psi_p$, $\overline{\beta}_+=\frac{i_0L|\Lambda|}{eD}$, $\overline{\beta}_\psi=\frac{F}{RT}\frac{i_{ps}L|\Lambda|}{\sigma_{ref}}$, $\overline{\beta}_s=\frac{i_0L|\Lambda|}{eM_s}$, $\eta^0=\Psi_s-\Psi_p$, $U^0=2.17+\frac{RT}{F}\left(-0.000558C_s\big|_{I^{\epsilon_p}}+8.1\right)$, *and the material's correction tensors* $\hat\kappa=\{\overline{\kappa}_{ij}\}_{i,j=1}^d$, $\hat{\mathbb{M}}=\{\overline{m}_{ij}\}_{i,j=1}^d$, $\hat{\mathbb{D}}=\{\overline{d}_{ij}\}_{i,j=1}^d$, $\hat\varepsilon=\{\overline{\varepsilon}_{ij}\}_{i,j=1}^d$, $\hat\Sigma=\{\overline{\sigma}_{ij}\}_{i,j=1}^d$, *and* $\hat{\mathbb{M}}_s=\{\overline{m}^s_{ij}\}_{i,j=1}^d$ *are defined by*

$$\begin{aligned}
&\overline{\kappa}_{ij}:=-\frac{1}{\mu|Y_D|}\int_{Y_D^p}w_i^j(\mathbf{y})\,d\mathbf{y}, && \overline{\varepsilon}_{ik}=\frac{1}{|Y|}\int_{Y_p}\lambda_D\left(\delta_{ik}-\delta_{ij}\frac{\partial\xi_\psi^k(\mathbf{y})}{\partial y_j}\right)d\mathbf{y},\\
&\overline{m}_{ik}:=\frac{1}{|Y|}\int_{Y_p}\delta_{ij}(\mathbf{y})\left(\delta_{ik}-\delta_{ij}\frac{\partial\xi_\psi^k(\mathbf{y})}{\partial y_j}\right)d\mathbf{y}, && \overline{m}^s_{ik}=\frac{1}{|Y|}\int_{Y_s}\delta_{ij}(\mathbf{y})\left(\delta_{ik}-\delta_{ij}\frac{\partial\xi_\phi^k(\mathbf{y})}{\partial y_j}\right)d\mathbf{y},\\
&\overline{d}_{ik}:=\frac{1}{|Y|}\int_{Y_p}d_{ij}(\mathbf{y})\left(\delta_{ik}-\delta_{ij}\frac{\partial\xi_\pm^k(\mathbf{y})}{\partial y_j}\right)d\mathbf{y}, && \overline{\sigma}_{ik}=\frac{1}{|Y|}\int_{Y_s}\sigma\left(\delta_{ik}-\delta_{ij}\frac{\partial\xi_\psi^k(\mathbf{y})}{\partial y_j}\right)d\mathbf{y}.
\end{aligned}\tag{3.40}$$

The correctors w_i^j, ξ_ψ^k, ξ_ϕ^k, *and* ξ^k *solve the reference cell problems (3.48),* $(3.63)_2$, *(3.72), and* $(3.63)_1$, *respectively.*

Before we derive these effective macroscopic formulation, we provide values for the parameters used in general Li batteries, see Tab. 2.

Table 2: Summary of available material parameters to model composite cathodes.

Parameter	**Value range**[(a)]	**Name**
L	$\approx 100-1000\mu m$	thickness of cathode
ℓ	$\approx 1\mu m$	radius of cathode particles/size of reference cell
λ_D	$<1nm$ [(d)]	Debye length
$D=D_\pm$	$\approx 1.5-4.5\times 10^{-10} m^2/s$ [(b)]	diffusion coeff. in $D_p^{\epsilon_p}$
$D_s=k_BTM_s$	$\approx 5.0\times 10^{-13}$	diffusion coeff. in $D_s^{\epsilon_p}$
σ	$\approx 1.0\times 10^4 S/m$	conductivity in $D_s^{\epsilon_p}$
α_a, α_c	0.5	transfer coefficients
c_{sm}	$\approx 29000 mol/m^3$	max. concentration in $D_s^{\epsilon_p}$
c_{pm}	$\approx 3920 mol/m^3$	max. concentration in $D_p^{\epsilon_p}$
k_{fb}	$\approx 10^{-10} m^4/(mol\cdot s)$	reaction rate at I^{ϵ_p}
i_{ps}	$\approx 12.6 A/m^2$	exchange current density
$\lvert\Lambda\rvert$	$\approx 5-15\times 10^3 m^2/kg$ [(c)]	specific interfacial/surface area (BET)

[(a)] Doyle et al. [14] & Garcia et al. [19], [(b)] Capiglia et al. [9], [(c)] Choy et al. [11], [(d)] Rademaker et al. [37]

3.1 Derivation of the upscaled cathode equations (3.39).

As the upscaling involves several equations, we will start with the Stokes equations driven by a Coulomb force $\mathbf{f}^{\epsilon_p}$. Then we consider the PNP system, and finally we look at the phase field equation describing the Li-intercalation process.

Homogenizing the generalized Stokes equations $(2.32)_1$:

Our derivation gives an extension of the classical formal homogenization result [23] towards Coulomb driving forces [24, 40, 41, 42].

Step 1: (Asymptotic expansion) We make the ansatz

$$\begin{aligned} \mathbf{u}^{\epsilon_D}(\mathbf{x}) &= \mathbf{U}(\mathbf{x},\mathbf{y}_D)+\epsilon_D\mathbf{u}^1(\mathbf{x},\mathbf{y}_D)+{\epsilon_D}^2\mathbf{u}^2(\mathbf{x},\mathbf{y}_D)+\cdots,\\ p^{\epsilon_D}(\mathbf{x}) &= P(\mathbf{x},\mathbf{y}_D)+\epsilon_D p^1(\mathbf{x},\mathbf{y}_D)+{\epsilon_D}^2 p^2(\mathbf{x},\mathbf{y}_D)+\cdots. \end{aligned} \tag{3.41}$$

The microscale $\mathbf{y}_D=\mathbf{x}/\epsilon_D\in Y_D$ is Y_D-periodic as in Section 2.2 where we introduced the microscopic formulation of the composite cathode based on a reference $FePO_4$-particle configuration Y and a reference flow/filtration cell Y_D.

We insert (3.41) into (2.32). This leads to the following problem where we only state the leading order terms,

$$\begin{aligned} -{\epsilon_D}^{-1}\nabla_{\mathbf{y}} P(\mathbf{x},\mathbf{y}_D) \\ +{\epsilon_D}^{0}\left\{\mu\Delta_{\mathbf{y}_D}\mathbf{U}(\mathbf{x},\mathbf{y}_D)-\left(\nabla_{\mathbf{y}_D}p^1(\mathbf{x},\mathbf{y}_D)+\nabla_{\mathbf{x}}P(\mathbf{x},\mathbf{y}_D)\right)\right\} \\ +{\epsilon_D}^{1}(\ldots)+\text{h.o.t.}=\mathbf{f}^{\epsilon_p}=-e\left(z_+c_+^{\epsilon_p}-z_-c_-^{\epsilon_p}\right)\nabla\phi_p^{\epsilon_p}, \qquad \text{in } Y_D^p, \end{aligned} \tag{3.42}$$

$$\begin{aligned} {\epsilon_D}^{-1}\text{div}_{\mathbf{y}_D}\mathbf{U}(\mathbf{x},\mathbf{y}_D) \\ +{\epsilon_D}^{0}\left(\text{div}_{\mathbf{y}_D}\mathbf{u}^1(\mathbf{x},\mathbf{y}_D)+\text{div}_{\mathbf{x}}\mathbf{U}(\mathbf{x},\mathbf{y}_D)\right) \\ +{\epsilon_D}^{1}(\ldots)+\text{h.o.t.}=0, \qquad \text{in } Y_D^p, \end{aligned} \tag{3.43}$$

$$\begin{aligned} {\epsilon_D}^{0}\mathbf{U}(\mathbf{x},\mathbf{y}_D) \\ +\epsilon_D\mathbf{u}^1(\mathbf{x},\mathbf{y}_D)+\text{h.o.t.}=\mathbf{0} \qquad \text{on } I_0. \end{aligned} \tag{3.44}$$

The variable $I_0 := \partial Y_D^p \cap \partial Y_D^p$ denotes the solid-pore interface on the level of the referenc cell Y_D. Higher order terms are referred to by h.o.t..

Step 2: (Comparing terms of equal order) The lowest order problem in Step 1 is obtained by comparing coefficients of the terms of order ${\epsilon_D}^{-1}$, i.e., we obtain the equations

$$\begin{aligned} \nabla_{\mathbf{y}_D}P(\mathbf{x},\mathbf{y}_D)=\mathbf{0}, \qquad \text{in } Y_D^p, \\ \text{div}_{\mathbf{y}_D}\mathbf{U}(\mathbf{x},\mathbf{y}_D)=0, \qquad \text{in } Y_D^p. \end{aligned} \tag{3.45}$$

This allows us to conclude that the leading order pressure component P is independent of the microscale $\mathbf{y}_D$ but not for leading order fluid velocity $\mathbf{U}$.

At the next order $\mathcal{O}({\epsilon_D}^0)$, we obtain

$$\begin{aligned} -\mu\Delta_{\mathbf{y}_D}\mathbf{U}(\mathbf{x},\mathbf{y}_D)+\left(\nabla_{\mathbf{y}_D}p^1(\mathbf{x},\mathbf{y}_D)+\nabla_{\mathbf{x}}P(\mathbf{x},\mathbf{y}_D)\right)=\mathbf{f}^{\epsilon_p}=-e\left(z_+c_+^{\epsilon_p}-z_-c_-^{\epsilon_p}\right)\nabla\phi_p^{\epsilon_p}, \qquad \text{in } Y_D^p, \\ \text{div}_{\mathbf{y}_D}\mathbf{u}^1(\mathbf{x},\mathbf{y}_D)+\text{div}_{\mathbf{x}}\mathbf{U}(\mathbf{x},\mathbf{y}_D)=0, \qquad \text{in } Y_D^p. \end{aligned} \tag{3.46}$$

Step 3: (Ansatz for first order terms) This step is not entirely standard and requires physical intuition. Making the usual ansatz for the pressure p^1 in the asymptotic expansion and treating the the fluid velocity $\mathbf{U}$ instead of $\mathbf{u}^1$ in the same way, which is motivated by its dependence on the microscale $\mathbf{y}_D$, i.e.,

$$\begin{aligned} p^1(\mathbf{x},\mathbf{y}_D)=\sum_{j=1}^{d}\left(\text{f}_j^{\epsilon_p}-\frac{\partial P(\mathbf{x})}{\partial x_j}\right)\pi^j(\mathbf{y}_D), \\ \mathbf{U}(\mathbf{x},\mathbf{y}_D)=\frac{1}{\mu}\sum_{j=1}^{d}\left(\text{f}_j^{\epsilon_p}-\frac{\partial P(\mathbf{x})}{\partial x_j}\right)\mathbf{w}^j(\mathbf{y}_D), \end{aligned} \tag{3.47}$$

then problem $(3.46)_1$ turns into the following

$$\text{(Cell Problem)} \quad \begin{cases} -\Delta_{\mathbf{y}_D}\mathbf{w}^j(\mathbf{y}_D)+\nabla_{\mathbf{y}_D}\pi^j(\mathbf{y}_D)=\mathbf{e}_j, & \text{in } Y_D^p, \\ \text{div}_{\mathbf{y}_D}\mathbf{w}^j(\mathbf{y}_D)=0, & \text{in } Y_D^p, \\ \mathbf{w}^j(\mathbf{y}_D)=0, & \text{on } I_0, \end{cases} \tag{3.48}$$

via ansatz $(3.47)_2$ as well as into Darcy's law after integrating $(3.47)_2$ over the pore space Y_D^p, i.e.,

$$\mathbf{V}(\mathbf{x},t) = \frac{|Y_D^p|}{|Y_D|} M_{Y_D^p}(\mathbf{U}(\mathbf{x},\mathbf{y}_D)) = -\frac{1}{\mu}\hat{\kappa}\left(\mathbf{f}^{\epsilon_p} - \nabla_{\mathbf{x}} P(\mathbf{x})\right), \tag{3.49}$$

where the hydraulic conductivity/permeability tensor $\hat{\kappa} := \{\kappa_{ij}\}_{i,j=1}^d$ is defined by the volume average

$$\kappa_{ij} = -\frac{1}{\mu}\frac{1}{|Y_D|}\int_{Y_D^p} w_i^j(\mathbf{y}_D)\, d\mathbf{y}_D\,. \tag{3.50}$$

It leaves to show that the effective Darcy velocity $\mathbf{V}$ is divergence free, that means, that it satisfies $(2.32)_2$. To this end, we can make use of equation $(3.46)_2$, which leads after integration over the pore space Y_D^p and with the help of Gauss' theorem to

$$\mathrm{div}_{\mathbf{x}}\,\mathbf{V}(\mathbf{x}) = \int_{\partial Y_D} \mathbf{n}\cdot\mathbf{u}^1(\mathbf{x},\mathbf{y}_D)\, do(\mathbf{y}_D) - \int_{I_0} \mathbf{n}\cdot\mathbf{u}^1(\mathbf{x},\mathbf{y}_D)\, do(\mathbf{y}_D) = 0, \tag{3.51}$$

where we used the Y_D-periodicity and the homogeneous boundary condition (3.44) at order $\mathcal{O}(\epsilon_D)$.

Finally, we note that once we have the upscaling result for the transport equations (2.33), which are formulated with respect to the pore scale l_p, then we can also determine the upscaled form of the Coulomb force term $\mathbf{f}^{\epsilon_p}$ by $\mathbf{f}^0$, i.e., by formally passing $\epsilon_p \to 0$. □

Homogenizing the PNP system:

The following derivation relies on homogenization results for the PNP system obtained in the context of microfluidics and soil mechanics such as [42, 43, 45]. The subsequent statements extend the derviation in [43] to include fluid flow.

Step 1: (Asymptotic expansion) We consider the asymptotic two-scale expansions

$$\begin{aligned} c_{\epsilon_p}^{\pm}(t,\mathbf{x}) &= C^{\pm}(t,\mathbf{x},\mathbf{y}) + \epsilon_p c_1^{\pm}(t,\mathbf{x},\mathbf{y}) + \epsilon_p^2 c_2^{\pm}(t,\mathbf{x},\mathbf{y}) + \text{h.o.t.}, \\ \psi_{\epsilon_p}(t,\mathbf{x}) &= \Psi(t,\mathbf{x},\mathbf{y}) + \epsilon_p \psi_1(t,\mathbf{x},\mathbf{y}) + \epsilon_p^2 \psi_2(t,\mathbf{x},\mathbf{y}) + \text{h.o.t.}. \end{aligned} \tag{3.52}$$

For notational convenience, we introduce for smooth enough functions v_{ϵ_p} the following operators,

$$\begin{aligned} \mathcal{A}_s v_{\epsilon_p}(\mathbf{x}) &:= -\sum_{i,j=1}^N \frac{\partial}{\partial x_i}\left(\varepsilon(\mathbf{x}/\epsilon_p)\delta_{ij}\frac{\partial v_{\epsilon_p}}{\partial x_j}\right) \\ &= \left[\left({\epsilon_p}^{-2}\mathcal{A}_0 + {\epsilon_p}^{-1}\mathcal{A}_1 + \mathcal{A}_2\right) v_{\epsilon_p}\right](\mathbf{x},\mathbf{x}/\epsilon_p), \\ \mathcal{B}_s^{\pm} v_{\epsilon_p}(\mathbf{x}) &:= -\sum_{i,j=1}^N \frac{\partial}{\partial x_i}\left(\delta_{ij}\frac{\partial v_{\epsilon_p}}{\partial x_j}\right) \\ &= \left[\left({\epsilon_p}^{-2}\mathcal{B}_0^{\pm} + {\epsilon_p}^{-1}\mathcal{B}_1^{\pm} + \mathcal{B}_2^{\pm}\right) v_{\epsilon_p}\right](\mathbf{x},\mathbf{x}/\epsilon_p), \\ \mathcal{B}_s^3 v_{\epsilon_p}(\mathbf{x}) &:= -\sum_{i,j=1}^N \frac{\partial}{\partial x_i}\left(v_{\epsilon_p}\delta_{ij}\frac{\partial v_{\epsilon_p}}{\partial x_j}\right) \\ &= \left[\left({\epsilon_p}^{-2}\mathcal{B}_0^3 + {\epsilon_p}^{-1}\mathcal{B}_1^3 + \mathcal{B}_2^3\right) v_{\epsilon_p}\right](\mathbf{x},\mathbf{x}/\epsilon_p), \end{aligned} \tag{3.53}$$

where $\mathcal{A}_i$ are related to the Poisson equation and are defined by,

$$\begin{aligned}
\mathcal{A}_0 &:= -\sum_{i,j=1}^{d} \frac{\partial}{\partial y_i}\left(\varepsilon(\mathbf{y})\delta_{ij}\frac{\partial}{\partial y_j}\right),\\
\mathcal{A}_1 &:= -\sum_{i,j=1}^{d} \frac{\partial}{\partial x_i}\left(\varepsilon(\mathbf{y})\delta_{ij}\frac{\partial}{\partial y_j}\right) - \sum_{i,j=1}^{d} \frac{\partial}{\partial y_i}\left(\varepsilon(\mathbf{y})\delta_{ij}\frac{\partial}{\partial x_j}\right),\\
\mathcal{A}_2 &:= -\sum_{i,j=1}^{d} \frac{\partial}{\partial x_i}\left(\varepsilon(\mathbf{y})\delta_{ij}\frac{\partial}{\partial x_j}\right),
\end{aligned} \tag{3.54}$$

The operators $\mathcal{B}_i^{\pm}$ and $\mathcal{B}_i^3$ related to the Nernst-Planck equations are defined for $c_\pm$ by,

$$\begin{aligned}
\mathcal{B}_0^{\pm} &:= -\sum_{i,j=1}^{d} \frac{\partial}{\partial y_i}\left(\delta_{ij}\frac{\partial}{\partial y_j}\right),\\
\mathcal{B}_1^{\pm} &:= -\sum_{i,j=1}^{d} \frac{\partial}{\partial x_i}\left(\delta_{ij}\frac{\partial}{\partial y_j}\right) - \sum_{i,j=1}^{d} \frac{\partial}{\partial y_i}\left(\delta_{ij}\frac{\partial}{\partial x_j}\right),\\
\mathcal{B}_2^{\pm} &:= -\sum_{i,j=1}^{d} \frac{\partial}{\partial x_i}\left(\delta_{ij}\frac{\partial}{\partial x_j}\right),\\
\mathcal{B}_0^{3} &:= -z_\pm \sum_{i,j=1}^{d} \frac{\partial}{\partial y_i}\left(\delta_{ij}\frac{\partial \Psi}{\partial y_j}\right),\\
\mathcal{B}_1^{3} &:= -z_\pm \sum_{i,j=1}^{d} \frac{\partial}{\partial x_i}\left(\delta_{ij}\frac{\partial \Psi}{\partial y_j}\right) - z_\pm \sum_{i,j=1}^{d} \frac{\partial}{\partial y_i}\left(\delta_{ij}\frac{\partial \Psi}{\partial x_j}\right) - z_\pm \sum_{i,j=1}^{d} \frac{\partial}{\partial y_i}\left(\delta_{ij}\frac{\partial \psi_1}{\partial y_j}\right),\\
\mathcal{B}_2^{3} &:= -\sum_{i,j=1}^{d} \frac{\partial}{\partial x_i}\left(\delta_{ij}\frac{\partial \Psi}{\partial x_j}\right) - z_\pm \sum_{i,j=1}^{d} \frac{\partial}{\partial x_i}\left(\delta_{ij}\frac{\partial \psi_1}{\partial y_j}\right)\\
&\quad - z_\pm \sum_{i,j=1}^{d} \frac{\partial}{\partial y_i}\left(\delta_{ij}\frac{\partial \psi_1}{\partial x_j}\right) - z_\pm \sum_{i,j=1}^{d} \frac{\partial}{\partial y_i}\left(\delta_{ij}\frac{\partial \psi_2}{\partial y_j}\right).
\end{aligned} \tag{3.55}$$

The definitions (3.53), (3.54), and (3.55) allow to immediately obtain the following sequence of problems by equating terms of equal power in ϵ_p, i.e.,

$$\mathcal{O}({\epsilon_p}^{-2}):\quad \begin{cases} \mathcal{B}_0^{\pm}C^{\pm} + \mathcal{B}_0^{3}C^{\pm} = 0 & \text{in } Y_p,\\ \quad C^{\pm} \text{ is } Y_p\text{-periodic}, & \\ \mathcal{A}_0\Psi = 0 & \text{in } Y,\\ \quad \Psi \text{ is } Y\text{-periodic}, & \end{cases} \tag{3.56}$$

$$\mathcal{O}({\epsilon_p}^{-1}):\quad \begin{cases} \left(\mathcal{B}_0^{\pm}+\mathcal{B}_0^{3}\right)c_1^{\pm} + Pe\,\mathrm{div}_{\mathbf{y}}\left(\mathbf{u}^{\epsilon_D}C^{\pm}\right) = -\left(\mathcal{B}_1^{\pm}+\mathcal{B}_1^{3}\right)C^{\pm} & \text{in } Y_p,\\ \quad c_1^{\pm} \text{ is } Y_p\text{-periodic}, & \\ \mathcal{A}_0\psi_1 = -\mathcal{A}_1\Psi & \text{in } Y,\\ \quad \psi_1 \text{ is } Y\text{-periodic}, & \end{cases} \tag{3.57}$$

$$\mathcal{O}(1)\colon\quad \begin{cases} \left(\mathcal{B}_0^{\pm}+\mathcal{B}_0^3\right)c_2^{\pm}+Pe\mathrm{div}_{\mathbf{y}}\left(\mathbf{u}^{\epsilon_D}c_1^{\pm}\right)=-\left(\mathcal{B}_1^{\pm}+\mathcal{B}_1^3\right)c_1^{\pm}-\left(\mathcal{B}_2^{\pm}+\mathcal{B}_2^3\right)C^{\pm} \\ \qquad\qquad -\partial_t C^{\pm}-Pe\mathrm{div}_{\mathbf{x}}(\mathbf{u}^{\epsilon_D}C^{\pm}) & \text{in } Y_p, \\ \quad c_2^{\pm} \text{ is } Y_p\text{-periodic}, & \\ \mathcal{A}_0\psi_2^3=(C^+-C^-)-\mathcal{A}_1\psi_1-\mathcal{A}_2\Psi & \text{in } Y, \\ \quad \psi_2 \text{ is } Y\text{-periodic}. \end{cases} \tag{3.58}$$

Using (3.54) and (3.55) we can rewrite (3.56) in the more intuitive form,

$$\begin{cases} -\Delta_{\mathbf{y}}C^+-\mathrm{div}_{\mathbf{y}}(C^+\nabla_{\mathbf{y}}\Psi)=0 & \text{in } Y_p, \\ -\Delta_{\mathbf{y}}C^--\mathrm{div}_{\mathbf{y}}(C^-\nabla_{\mathbf{y}}\Psi)=0 & \text{in } Y_p, \\ -\mathrm{div}_{\mathbf{y}}(\varepsilon(\mathbf{y})\nabla_{\mathbf{y}}\Psi)=0 & \text{in } Y. \end{cases} \tag{3.59}$$

Equation $(3.59)_3$ is classical in elliptic homogenization theory [6, 10, 12, 23]. Hence, we immediately can conclude that $\Psi(t,\mathbf{x})$ is independent of the microscale $\mathbf{y}\in Y$. Entering with this result into $(3.59)_1$ and $(3.59)_2$ further implies that also $C^{\pm}(t,\mathbf{x})$ and $\Psi(t,\mathbf{x})$ are independent of the microscale $\mathbf{y}\in Y_p$.

The next problem in the sequence, i.e., (3.57), has the following explicit form,

$$\begin{cases} -\Delta_y c_1^{\pm}-\mathrm{div}_{\mathbf{y}}(z_{\pm}C^{\pm}\nabla_{\mathbf{y}}\psi_1)+Pe\mathrm{div}_{\mathbf{y}}(\mathbf{u}^{\epsilon_D}C^{\pm})=\mathrm{div}_{\mathbf{y}}\left(z_{\pm}c_1^{\pm}\nabla_{\mathbf{y}}\Psi\right)+\mathrm{div}_{\mathbf{x}}\nabla_{\mathbf{y}}C^{\pm} \\ \qquad\qquad +\mathrm{div}_{\mathbf{x}}(z_{\pm}C^{\pm}\nabla_{\mathbf{y}}\Psi)+\mathrm{div}_{\mathbf{y}}\nabla_{\mathbf{x}}C^{\pm}+\mathrm{div}_{\mathbf{y}}(z_{\pm}C^{\pm}\nabla_{\mathbf{x}}\Psi) & \text{in } Y_p, \\ -\mathrm{div}_{\mathbf{y}}(\varepsilon(\mathbf{y})\nabla_{\mathbf{y}}\psi_1)=\mathrm{div}_{\mathbf{x}}(\varepsilon(\mathbf{y})\nabla_{\mathbf{y}}\Psi)+\mathrm{div}_{\mathbf{y}}(\varepsilon(\mathbf{y})\nabla_{\mathbf{x}}\Psi) & \text{in } Y, \end{cases} \tag{3.60}$$

where the convective terms $Pe\mathrm{div}_{\mathbf{y}}(\mathbf{u}^{\epsilon_D}C^{\pm})$ disappear since $C^{\pm}$ and $\mathbf{u}^{\epsilon_D}$ are both independent of $\mathbf{y}$. The independence of $C^{\pm}$ and Ψ from $\mathbf{y}$ together with the linearity of (3.60) motivates to make the following ansatz,

$$c_1^{\pm}(t,\mathbf{x},\mathbf{y})=-\sum_{j=1}^{d}\xi_{\pm}^j(\mathbf{y})\frac{\partial C^{\pm}(t,\mathbf{x})}{\partial x_j},\quad\text{and}\quad \psi_1(t,\mathbf{x},\mathbf{y})=-\sum_{j=1}^{d}\xi_{\psi}^j(\mathbf{y})\frac{\partial\Psi(t,\mathbf{x})}{\partial x_j},. \tag{3.61}$$

With the local thermodynamic equilibrium property, i.e.,

$$0=\frac{\partial}{\partial x_j}\log C^{\pm}\pm z_{\pm}\frac{\partial}{\partial x_j}\Psi, \tag{3.62}$$

we can simplify (3.60) to,

$$\begin{cases} -\sum_{i,j=1}^{N}\frac{\partial}{\partial y_i}\left(\delta_{ij}\frac{\partial}{\partial y_j}\left(\xi_{\pm}^j(\mathbf{y})-y_i\right)\right)=-\sum_{i,j=1}^{N}\frac{\partial}{\partial y_i}\left(\delta_{ij}\frac{\partial}{\partial y_j}\left(\xi_{\psi}^j(\mathbf{y})-y_i\right)\right) & \text{in } Y_p, \\ \quad \xi_{\pm}^j(\mathbf{y}) \text{ is } Y_p\text{-periodic and } \mathcal{M}_{Y_p}(\xi_{\pm}^j)=0, & \\ -\sum_{i,j=1}^{N}\frac{\partial}{\partial y_i}\left(\varepsilon(\mathbf{y})\delta_{ij}\frac{\partial}{\partial y_j}\left(\xi_{\psi}^j(\mathbf{y})-y_i\right)\right)=0 & \text{in } Y, \\ \quad \xi_{\psi}^j(\mathbf{y}) \text{ is } Y\text{-periodic and } \mathcal{M}_Y(\xi_{\psi}^j)=0. & \end{cases} \tag{3.63}$$

System (3.63) defines the reference cell problems for the upscaled Poisson-Nernst-Planck equations describing binary symmetric electrolytes in porous media. Thanks to the simplification of (3.60) via (3.62), the well-posedness of (3.63) follows by Lax-Milgram's theorem.

The last problem (3.58) is again well-posed by Lax-Milgram's theorem or the Fredholm alternative. A necessary and sufficient condition for the existence and uniqueness of solutions to (3.63) is the requirement that corresponding right-hand sides are zero after integrating over Y_p. Hence, we immediately obtain,

$$\textbf{porous media PNP:}\quad \begin{cases} |Y_p|\,\partial_t C^{\pm} + Pe\,|Y_p|\,\mathrm{div}_{\mathbf{x}}(\mathbf{u}^{\epsilon_D} C^{\pm}) - \sum_{i,j,k=1}^{d} \left(\frac{\partial}{\partial x_i}\left(\delta_{ik} - \delta_{ij}\frac{\partial \xi_{\pm}^k}{\partial y_j}\right)\frac{\partial C^{\pm}}{\partial x_k}, 1\right)_{Y_p} \\ \qquad\qquad - \sum_{i,j,k=1}^{d} \left(\frac{\partial}{\partial x_i}\left(z_{\pm} C^{\pm}\left\{ \delta_{ik} - \delta_{ij}\frac{\partial \xi_{\psi}^k}{\partial y_j}\right\}\frac{\partial \Psi}{\partial x_k}\right), 1\right)_{Y_p} = 0\,, \\ -\sum_{i,j,k=1}^{d} \left(\frac{\partial}{\partial x_i}\left(\varepsilon(\mathbf{y})\left\{ \delta_{ik} - \delta_{ij}\frac{\partial \xi_{\psi}^k}{\partial y_j}\right\}\frac{\partial \Psi}{\partial x_k}\right), 1\right)_{Y} = |Y_p|\,(C^+ - C^-)\,. \end{cases} \tag{3.64}$$

We note that $\mathbf{u}^{\epsilon_D}$ is not upscaled/homogenized here since this allows us to account for multiple scales such as the pore scale l_p, the Darcy scale l_D, and the macroscale L. For details regarding the verifaction of the cell problems with Lax-Milgram's theorem or the Fredholm alternative [12], we refer the interested reader also to [44] where these tools are applied in a related problem by a modified asymptotic expansion.

It leaves to homogenize the right-hand side of the Stokes equations (2.32), which is scaled with respect to the pore scale l_p. With the corrector ξ_{ψ}^k we immediately obtain at the level $\mathcal{O}(\epsilon_p^0)$ that the effective Coulomb force term is $f^0 = -\eta(C_+ - C_-)\hat{\mathbb{M}}\nabla\Psi_p$ since at $\mathcal{O}(\epsilon_p^0)$ we have with (3.61)

$$-\eta(C_+ - C_-)(\nabla_{\mathbf{x}}\Psi_p + \nabla_{\mathbf{y}}\psi_1) = -\eta(C_+ - C_-)\left(\sum_{i,j,k=1}^{d} \left(\delta_{ik} - \delta_{ij}\frac{\partial \xi_{\psi}^k}{\partial y_j}\right)\frac{\partial \Psi_p}{\partial x_k}\right).$$

□

Homogenizing the phase field intercalation equation

Step 1: (Asymptotic expansion) The derivation of the phase field equations follows the essential steps presented in [47] and which we repeat here for the reader's convenience. The heterogeneity parameter $\epsilon = \epsilon_p$ is the pore scale as for the ionic transport in the polymer solution.

In the context of asymptotic two-scale expansions, the Laplace operator Δ can be written as follows,

$$\begin{aligned} &\mathcal{A}_0 = -\sum_{i,j=1}^{d} \frac{\partial}{\partial y_i}\left(\delta_{ij}\frac{\partial}{\partial y_j}\right)\,, \quad \mathcal{A}_1 = -\sum_{i,j=1}^{d}\left[\frac{\partial}{\partial x_i}\left(\delta_{ij}\frac{\partial}{\partial y_j}\right) + \frac{\partial}{\partial y_i}\left(\delta_{ij}\frac{\partial}{\partial x_j}\right)\right], \\ &\mathcal{A}_2 = -\sum_{i,j=1}^{d} \frac{\partial}{\partial x_j}\left(\delta_{ij}\frac{\partial}{\partial x_j}\right), \end{aligned} \tag{3.65}$$

such that we can identify $\mathcal{A}_\epsilon := \epsilon^{-2}\mathcal{A}_0 + \epsilon^{-1}\mathcal{A}_1 + \mathcal{A}_2 = \Delta$. We account for the multiscale nature of strongly heterogeneous environments [43, 23, 31] by the following ansatz

$$\eta^{\epsilon} \approx \eta_0(\mathbf{x},\mathbf{y},t) + \epsilon\eta_1(\mathbf{x},\mathbf{y},t) + \epsilon^2\eta_2(\mathbf{x},\mathbf{y},t) + \ldots\,, \quad \text{for} \quad \eta \in \{w,\phi\}\,. \tag{3.66}$$

Before we can insert (3.66) into the microscopic formulation (2.34), we approximate the derivative of the nonlinear homogeneous free energy density f_r by a Taylor expansion around the homogenized order parameter ϕ_0, that means,

$$f_r(\phi^{\epsilon}) \approx f_r(\phi_0) + f_r'(\phi_0)(\phi^{\epsilon} - \phi_0) + \frac{1}{2}f_r''(\phi_0)(\phi^{\epsilon} - \phi_0)^2 + \mathcal{O}\left((\phi^{\epsilon} - \phi_0)^3\right), \tag{3.67}$$

where ϕ_0 denotes the leading-order term in (3.66). Substituting (3.66) and (3.67) into (2.34), which we split into two second order problems as suggested in [46], and using (3.65) provides the following sequence of problems

$$\mathcal{O}(\epsilon^{-2}):\quad \begin{cases} \mathcal{A}_0[\lambda w_0 + f_r(\phi_0)] = 0 & \text{in } Y_s, \\ \quad \text{under no flux b.c. and with } w_0 \text{ is } Y_s\text{-periodic}, & \\ \mathcal{A}_0\phi_0 = 0 & \text{in } Y_s, \\ \quad \text{with } \mathbf{n}_{sp}\cdot\nabla\phi_0 = 0 \text{ on } \partial Y_s^w := \partial Y_s \cap \partial Y_p \text{ and } \phi_0 \ Y_s\text{-periodic}, & \end{cases} \tag{3.68}$$

$$\mathcal{O}(\epsilon^{-1}):\quad \begin{cases} \mathcal{A}_0[\lambda w_1 + f_r'(\phi_0)\phi_1] = -\mathcal{A}_1[\lambda w_0 + f_r(\phi_0)] & \text{in } Y_s, \\ \quad \text{under no flux b.c. and } w_1 \ Y_s\text{-periodic}, & \\ \mathcal{A}_0\phi_1 = -\mathcal{A}_1\phi_0 & \text{in } Y_s, \\ \quad \text{with } \mathbf{n}_{sp}\cdot\nabla\phi_1 = 0 \text{ on } \partial Y_s \cap \partial Y_p \text{ and } \phi_1 \ Y_s\text{-periodic}, & \end{cases} \tag{3.69}$$

$$\mathcal{O}(\epsilon^{0}):\quad \begin{cases} \mathcal{A}_0\left[\lambda w_2 + \left(\frac{1}{2}f_r''(\phi_0)\phi_1^2 + f_r'(\phi_0)\phi_2\right)\right] & \\ \qquad = -\left(\mathcal{A}_2[\lambda w_0 + f_r(\phi_0)] + \mathcal{A}_1[\lambda w_1 - f_r'(\phi_0)\phi_1]\right) & \\ \qquad\qquad -\partial_t\mathcal{A}_2^{-1}w_0 & \text{in } Y_s, \\ \quad \text{under no flux b.c. and with } w_2 \ Y_s\text{-periodic}, & \\ \mathcal{A}_0\phi_2 = -\mathcal{A}_2\phi_0 - \mathcal{A}_1\phi_1 + w_0 & \text{in } Y_s, \\ \quad \text{with } \mathbf{n}_{sp}\cdot\nabla\phi_2 = g_\epsilon \text{ on } \partial Y_s \cap \partial Y_p \text{ and } \phi_2 \ Y_s\text{-periodic}. & \end{cases} \tag{3.70}$$

Step 2: (Analysis of the sequence of problems) The first problem (3.68) immediately implies that the leading-orders ϕ_0 and w_0 are independent of the microscale $\mathbf{y}$ [43, 31]. This suggests the following ansatz for w_1 and ϕ_1, i.e.,

$$w_1(\mathbf{x},\mathbf{y},t) = -\sum_{k=1}^{d}\xi_w^k(\mathbf{y})\frac{\partial w_0}{\partial x_k}(\mathbf{x},t), \quad \phi_1(\mathbf{x},\mathbf{y},t) = -\sum_{k=1}^{d}\xi_\phi^k(\mathbf{y})\frac{\partial \phi_0}{\partial x_k}(\mathbf{x},t) = \phi_1(\mathbf{x},\mathbf{y},t). \tag{3.71}$$

Inserting (3.71) into $(3.69)_2$ provides an equation for the correctors ξ_w^k and ξ_ϕ^k. The resulting equation for ξ_ϕ^k can be immediately written for $1 \le k \le d$ as,

$$\xi_\phi^k:\quad \left\{ -\textstyle\sum_{i,j=1}^{d}\frac{\partial}{\partial y_i}\left(\delta_{ik} - \delta_{ij}\frac{\partial \xi_\phi^k}{\partial y_j}\right) = -\mathrm{div}\left(\mathbf{e}_k - \nabla_y\xi_\phi^k\right) = 0 \quad \text{in } Y_s, \right. \tag{3.72}$$

for $\xi_\phi^k(\mathbf{y})$ Y-periodic with $\mathcal{M}_{Y_s}(\xi_\phi^k) = 0$ and associated boundary condition $\mathbf{n}\cdot\left(\nabla\xi_\phi^k + \mathbf{e}_k\right) = 0$ on $\partial Y_s^w := \partial Y_s \cap \partial Y_p$.

To study $(3.69)_1$, we first rewrite $\mathcal{B}_0[f_r'(\phi_0)\phi_1]$ and $\mathcal{B}_1 f_r(\phi_0)$ as follows

$$\mathcal{A}_0[f_r'(\phi_0)\phi_1] = -\sum_{k,i,j=1}^{d}\frac{\partial}{\partial y_i}\left(\delta_{ij}\frac{\partial\xi_\phi^k}{\partial y_j}\frac{\partial f_r(\phi_0)}{\partial x_k}\right), \quad \mathcal{A}_1 f_r(\phi_0) = \sum_{i,j=1}^{d}\frac{\partial}{\partial y_i}\left(\delta_{ij}\frac{\partial f_r(\phi_0)}{\partial x_j}\right). \tag{3.73}$$

Doing the same for w_1 and w_0 and using (3.71) leads then to

$$-\lambda\sum_{k,i,j=1}^{d}\frac{\partial}{\partial y_i}\left(\delta_{ij}\left(\frac{\partial x_k}{\partial x_j} - \frac{\partial\xi_w^k}{\partial y_j}\right)\frac{\partial w_0}{\partial x_k}\right) = \sum_{k,i,j=1}^{d}\frac{\partial}{\partial y_i}\left(\delta_{ij}\left(\frac{\partial x_k}{\partial x_j} - \frac{\partial\xi_\phi^k}{\partial y_j}\right)\frac{\partial f_r(\phi_0)}{\partial x_k}\right), \tag{3.74}$$

in Y_s. Since the chemical potential $\mu(\phi)=\frac{\delta E(\phi)}{\delta\phi}$ is locally in thermodynamic equilibrium, we finally obtain the reference cell problem for ξ_w^k, $1\le k\le d$, for given ξ_ϕ^k

$$\begin{cases} -\sum_{i,j=1}^d \frac{\partial}{\partial y_i}\left(\delta_{ik}-\delta_{ij}\frac{\partial \xi_w^k}{\partial y_j}\right) \\ \qquad\qquad =-\sum_{i,j=1}^d \frac{\partial}{\partial y_i}\left(\delta_{ik}-\delta_{ij}\frac{\partial \xi_\phi^k}{\partial y_j}\right) \quad \text{in } Y_s, \end{cases} \tag{3.75}$$

where $\xi_w^k(\mathbf{y})$ is Y-periodic with boundary condition $\sum_{i,j=1}^d \mathrm{n}_i\left(\left(\delta_{ij}\frac{\partial \xi_w^k}{\partial y_j}-\delta_{ik}\right)+\left(\delta_{ik}-\delta_{ij}\frac{\partial \xi_\phi^k}{\partial y_j}\right)\right)=0$ on $\partial Y_s^w=\partial Y_s\cap\partial Y_p$ and $\mathcal{M}_{Y_s}(\xi_w^k)=0$.

Step 3: (Second order problem: upscaled equation) The last problem (3.70) then gives the upscaled equations by a solvability constraint, i.e., the Fredholm alternative. Hence, the solvability of $(3.70)_2$ is achieved by setting

$$-\sum_{i,k=1}^d\left[\sum_{j=1}^d\int_{Y_s}\left(\delta_{ik}-\delta_{ij}\frac{\partial\xi_\phi^k}{\partial y_j}\right)d\mathbf{y}\right]\frac{\partial^2\phi_0}{\partial x_i\partial x_k}=|Y_s|\,w_0+\tilde{g}_0\,. \tag{3.76}$$

where $\tilde{g}_0:=-\frac{\gamma}{C_h}\int_{\partial Y_s^w}\left(a_1\chi_{\partial Y_s^{w_1}}+a_2\chi_{\partial Y_s^{w_2}}\right)do(\mathbf{y})$ and $\partial Y_s^w=\partial Y_s^{w_1}\cup\partial Y_s^{w_2}$. (3.76) can be written compactly as $-\Delta_{\hat{\mathbb{M}}_s}\phi_0:=-\mathrm{div}\left(\hat{\mathbb{M}}_s\nabla\phi_0\right)=qw_0+\tilde{g}_0$ by $(3.40)_4$. Applying the same ideas to equation $(3.70)_1$ leads to

$$\int_{Y_s}\left\{-\lambda(\mathcal{A}_2w_0+\mathcal{A}_1w_1)-\frac{1}{\lambda}\mathcal{A}_1[f_r'(\phi_0)\phi_1]-\frac{1}{\lambda}\mathcal{A}_2f_r(\phi_0)-\partial_t\mathcal{A}_2^{-1}w_0\right\}d\mathbf{y}=0\,, \tag{3.77}$$

where the first two terms can be rewritten with (3.75) by $\int_{Y_s}-(\mathcal{A}_2w_0+\mathcal{A}_1w_1)\,d\mathbf{y}=\mathrm{div}\left(\hat{\mathbb{M}}_s\nabla w_0\right)$.The third integrand in (3.77) becomes $-\mathcal{A}_1[f_r'(\phi_0)\phi_1]=-\sum_{i,j=1}^d\delta_{ij}\sum_{k=1}^d\frac{\partial\xi_\phi^k}{\partial y_j}\frac{\partial^2 f_r(\phi_0)}{\partial x_k\partial x_i}$, where we applied the chain rule $\frac{\partial^2 f_r(\phi_0)}{\partial x_k\partial x_j}=f_r''(\phi_0)\frac{\partial\phi_0}{\partial x_k}\frac{\partial\phi_0}{\partial x_j}+f_r'(\phi_0)\frac{\partial^2\phi_0}{\partial x_k\partial x_j}$ and integration by parts. Adding now the term $-\mathcal{A}_2f(\phi_0)$ and using (3.72) finally gives $-\mathcal{A}_1[f_r'(\phi_0)\phi_1]-\mathcal{A}_2f_r(\phi_0)=\mathrm{div}\left(\hat{\mathbb{M}}_s\nabla f_r(\phi_0)\right)$.

These considerations finally lead to the following effective equation for ϕ_0, i.e.,

$$q\frac{\partial\phi_0}{\partial t}=\mathrm{div}\left(\hat{\mathbb{M}}_s\nabla f_r(\phi_0)\right)+\frac{\lambda}{q}\mathrm{div}\left(\hat{\mathbb{M}}_s\nabla\left(\mathrm{div}\left(\hat{\mathbb{M}}_s\nabla\phi_0\right)-\frac{1}{\lambda}\tilde{g}_0\right)\right). \tag{3.78}$$

In the case where the homogeneous free energy F_r is the classical double-well potential $F_r(\phi)=1/4(\phi^2-1)^2$, one can verify the solvability of (3.78) along with the arguments in [33]. □

4 Discussion and conclusions

We have given a short summary of widely used charge transport formulations in Li-ion battery systems. Based on well-accepted microscopic composite cathode equations which take into account ionic transport in the polymer electrolyte, electron transport as well as Li-intercalation undergoing a possible phase transformation in the solid phase, and Butler-Volmer reactions across the solid-electrolyte interface, we derived a novel upscaled/homogenized formulation. To the best of our knowledge, this seems to be the first two-scale asymptotic homogenization of composite cathodes

for Li-batteries that also accounts for thermodynamically relevant phase transformations of crystalline host materials such as $FePO_4$. For a literature overview on recent results available, we refer the interested reader to Tab. 1.

The promising feature of being able to account for three different scales, i.e., pore scale l_p, Darcy's scale l_D, and macroscale L, with the two-scale asymptotic expansion method by exploiting coupling of different physical processes, provides novel modelling opportunities not only in the context of batteries, but also in fuel cell systems, transport in porous media, and oil recovery for instance. We expect that the derived equations serve as a convenient computational model that allows to apply well-known numerical strategies available for homogeneous domains without ending up with high-dimensional discrete equations. Since the homogenization method is, compared to volume averaging, still less popular in applied sciences and engineering, we believe that the presented upscaling ideas and mathematical tools will become increasingly interesting in applications due to its reliable and systematic basis relying on rigorous convergence methods such as two-scale convergence [1, 32] or Gamma convergence, e.g. [13].

Acknowledgements

We acknowledge financial support from EPSRC Grant No EP/P011713/1.

References

[1] G. Allaire. Homogenization and two-scale convergence. *SIAM J. Math. Anal.*, 23(6):1482–1518, 1992.

[2] G. Allaire, A. Mikelic, and A. Piatnitski. Homogenization of the linearized ionic transport equations in rigid periodic porous media. *Journal of Mathematical Physics*, 51(12):123103, 2010.

[3] A.J. Bard and L.R. Faulkner. *Electrochemical Methods: Fundamentals and Applications*. Wiley, 2000.

[4] M.Z. Bazant. Theory of chemical kinetics and charge transfer based on nonequilibrium thermodynamics. *Accounts of Chemical Research*, 46(5):1144–1160, 2013. PMID: 23520980.

[5] D. Bedeaux, S. Kjelstrup, and H. C. Öttinger. Nonlinear coupled equations for electrochemical cells as developed by the general equation for nonequilibrium reversible-irreversible coupling. *The Journal of Chemical Physics*, 141(12), 2014.

[6] A. Bensoussan, J.-L. Lions, and G. Papanicolaou. *Asymptotic Analysis for Periodic Structures*. North-Holland Publishing Company, North-Holland, Amsterdam, 1978.

[7] D.A.G. Bruggeman. Berechnung verschiener physikalischer Konstanten von heterogenen Substanzen I. Dielektrizitaätskonstanten und Leitfähigkeiten der Mischköerper aus isotropen Substanzen. *Annalen der Physik*, 5(24):636–664, 1935.

[8] J.W. Cahn and J.E. Hilliard. Free Energy of a Nonuniform System. I. Interfacial Free Energy. *J. Chem. Phys.*, 28(2):258, 1958.

[9] C. Capiglia, Y. Saito, H. Kageyama, P. Mustarelli, T. Iwamoto, T. Tabuchi, and H. Tukamoto. ^{7}Li and ^{19}F diffusion coefficients and thermal properties of non-aqueous electrolyte solutions for rechargeable lithium batteries. *Journal of Power Sources*, 81-82:859–862, 1999.

[10] G.A. Chechkin, A.L. Piatnitski, and A.S. Shamaev. *Homogenization: Methods and Applications*. American Mathematical Society, 2007.

[11] S. Choy, Y.T. Lee, H.K. Park, S.M. Park, and J.E. Lee. Lithium iron phosphate having olivine structure and method for preparing the same. *US Patent App. 12/709,200*, 2010.

[12] D. Cioranescu and P. Donato. *An Introduction to Homogenization*, volume 17 of *Oxford Lecture Series in Mathematics and its Applications*. Oxford University Press, New York, 1999.

[13] G. Dal Maso. *An introduction to* Γ*-convergence*. Birkhauser, Basel, 1993.

[14] M. Doyle, T.F. Fuller, and J. Newman. Modeling of Galvanostatic Charge and Discharge of the Lithium/Polymer/Insertion Cell. *J. Electrochem. Soc.*, 140(6):1526, 1993.

[15] W. Dreyer, C. Guhlke, and R. Muller. Overcoming the shortcomings of the Nernst-Planck model. *Phys. Chem. Chem. Phys.*, 15:7075–7086, 2013.

[16] Y. Efendiev, O. Iliev, and V. Taralova. Upscaling of an isothermal li-ion battery model via the homogenization theory. *preprint*, 2013.

[17] B. Eisenberg, Y. Hyon, and C. Liu. Energy variational analysis of ions in water and channels: Field theory for primitive models of complex ionic fluids. *The Journal of Chemical Physics*, 133(10):104104, September 2010.

[18] C.M. Elliott, B. Stinner, V. Styles, and R. Welford. Numerical computation of advection and diffusion on evolving diffuse interfaces. *IMA Journal of Numerical Analysis*, 31(3):786–812, May 2010.

[19] R.E. García, Y.M. Chiang, W.C. Carter, P. Limthongkul, and C.M. Bishop. Microstructural modeling and design of rechargeable lithium-ion batteries. *J. Electrochem. Soc.*, 152(1):A255–A263, 2005.

[20] A. Gully, H. Liu, S. Srinivasan, A. K. Sethurajan, S. Schougaard, and B. Protas. Effective transport properties of porous electrochemical materials - a homogenization approach. *Journal of The Electrochemical Society*, 161(8):E3066–E3077, 2014.

[21] B.C. Han, A. Van der Ven, D. Morgan, and G. Ceder. Electrochemical modeling of intercalation processes with phase field models. *Electrochimica Acta*, 49(26):4691–4699, October 2004.

[22] G. Hautier, A. Jain, S.P. Ong, B. Kang, C. Moore, R. Doe, and G. Ceder. Phosphates as lithium-ion battery cathodes: An evaluation based on high-throughput ab initio calculations. *Chem. Mater.*, 23(15):3495–3508, 2011.

[23] U. Hornung. *Homogenization and Porous Media*. Interdisciplinary applied mathematics. Springer, 1997.

[24] J.W. Jerome. Analytical approaches to charge transport in a moving medium. *Transport Theory and Statistical Physics*, 31(4-6):333–366, January 2002.

[25] P.M. Kekenes-Huskey, A.K. Gillette, and J.A. McCammon. Predicting the influence of long-range molecular interactions on macroscopic-scale diffusion by homogenization of the smoluchowski equation. *The Journal of Chemical Physics*, 140(17), 2014.

[26] W. Lai and F. Ciucci. Mathematical modeling of porous battery electrodesRevisit of Newman's model. *Electrochimica Acta*, 56(11):4369–4377, April 2011.

[27] B. Li, B. Lu, Z. Wang, and J.A. McCammon. Solutions to a reduced poisson-nernst-planck system and determination of reaction rates. *Physica A*, 389(7):13291345, April 2010.

[28] R. Malik, F. Zhou, and G. Ceder. Kinetics of non-equilibrium lithium incorporation in $LiFePO_4$. *Nature Mater.*, 10:587–590, 2011.

[29] P.A. Markowich, C.A. Ringhofer, and C. Schmeiser. *Semiconductor equations*. Springer-Verlag, 1990.

[30] N. Meethong, H.-Y.S. Huang, W.C. Carter, and Y.-M. Chiang. Size-dependent lithium miscibility gap in nanoscale li1-x fepo4. *Electrochemical and Solid-State Letters*, 10(5):A134–A138, 2007.

[31] C.C. Mei and B. Vernescu. *Homogenization Methods for Multiscale Mechanics*. World Scientific, 2010.

[32] G. Nguetseng. A general convergence result for a functional related to the theory of homogenization. *SIAM J. Math. Anal.*, 20(3):608–623, 1989.

[33] A. Novick-Cohen. On cahn-hilliard type equations. *Nonlinear Anal-Theor.*, 15(9):797 – 814, 1990.

[34] L. Onsager. Reciprocal relations in irreversible processes I. *Phys. Rev.*, 37:405–426, 1931.

[35] L. Onsager. Reciprocal relations in irreversible processes II. *Phys. Rev.*, 38:2265–2279, 1931.

[36] R. L. Pego. Front migration in the nonlinear cahn-hilliard equation. *Proc. R. Soc. Lond. A*, 422(1863):261–278, 1989.

[37] T. J. Rademaker, G. R. A. Akkermans, D. L. Danilov, and P. H. L. Notten. On the deviation of electro-neutrality in li-ion battery electrolytes. *Journal of The Electrochemical Society*, 161(8):E3365–E3372, 2014.

[38] N. Ray, T. Noorden, F. Frank, and P. Knabner. Multiscale Modeling of Colloid and Fluid Dynamics in Porous Media Including an Evolving Microstructure. *Transport in Porous Media*, September 2012.

[39] G. Richardson, G. Denuault, and C.P. Please. Multiscale modelling and analysis of lithium-ion battery charge and discharge. *Journal of Engineering Mathematics*, 72(1):41–72, 2012.

[40] T. Roubicek. Incompressible ionized non-newtonian fluid mixtures. *SIAM J. Math. Anal.*, 39:863–890, 2007.

[41] M. Schmuck. Analysis of the NavierStokesNernstPlanckPoisson System. *Math. Mod. Meth. Appl. S.*, 19(06):993, 2009.

[42] M. Schmuck. Modeling and deriving porous media {S}tokes-{P}oisson-{N}ernst-{P}lanck equations by a multi-scale approach. *Commun. Math. Sci.*, 9(3):685–710, 2011.

[43] M. Schmuck. First error bounds for the porous media approximation of the Poisson-Nernst-Planck equations. *Z. Angew. Math. Mech.*, 92(4):304–319, 2012.

[44] M. Schmuck. New porous medium Poisson-Nernst-Planck equations for strongly oscillating electric potentials. *Journal of Mathematical Physics*, 54(2):021504, 2013.

[45] M. Schmuck and M.Z. Bazant. Homogenization of the poisson–nernst–planck equations for ion transport in charged porous media. *SIAM Journal on Applied Mathematics*, 75(3):1369–1401, 2015.

[46] M. Schmuck and P. Berg. Effective macroscopic equations for species transport and reactions in porous catalyst layers. *Journal of The Electrochemical Society*, 161(8):E3323–E3327, 2014.

[47] M. Schmuck, G.A. Pavliotis, and S. Kalliadasis. Effective macroscopic interfacial transport equations in strongly heterogeneous environments for general homogeneous free energies. *Appl. Math. Lett.*, 35:12–17, 2014.

[48] K.E. Thomas-Alyea and J. Newman. *Electrochemical Systems (Third Edition)*. John Wiley & Sons, Incorporated, 2010.

[49] J. van Brakel and P.M. Heertjes. ANALYSIS OF DIFFUSION IN MACROPOROUS MEDIA IN TERMS OF A POROSITY , A TORTUOSITY AND A CONSTRICTIVITY FACTOR XA RSA + XB / (MA CrB ˜. *Int. J. Heat Mass Transfer*, 17:1093–1103, 1974.

[50] K. West, T. Jacobsen, and S. Atlung. Modeling of porous insertion electrodes with liquid electrolyte. *J. Electrochem. Soc.*, 129(7):1480–1485, 1982.